

CrystEngComm

Accepted Manuscript



This is an *Accepted Manuscript*, which has been through the Royal Society of Chemistry peer review process and has been accepted for publication.

Accepted Manuscripts are published online shortly after acceptance, before technical editing, formatting and proof reading. Using this free service, authors can make their results available to the community, in citable form, before we publish the edited article. We will replace this *Accepted Manuscript* with the edited and formatted *Advance Article* as soon as it is available.

You can find more information about *Accepted Manuscripts* in the [Information for Authors](#).

Please note that technical editing may introduce minor changes to the text and/or graphics, which may alter content. The journal's standard [Terms & Conditions](#) and the [Ethical guidelines](#) still apply. In no event shall the Royal Society of Chemistry be held responsible for any errors or omissions in this *Accepted Manuscript* or any consequences arising from the use of any information it contains.

ARTICLE

Energetic Multi-component Molecular Solids of Tetrafluoroterephthalic Acid with Some Aza Compounds by Strong Hydrogen Bonds and Weak Intermolecular Interactions of C-H \cdots F and C-H \cdots O

Cite this: DOI: 10.1039/x0xx00000x

Received 00th January 2012,
Accepted 00th January 2012

DOI: 10.1039/x0xx00000x

www.rsc.org/

Lei Wang^{a*}, Yanjing Hu^a, Wenqiang Wang^a, Faqian Liu^a, and Keke Huang^{b*}

Tetrafluoroterephthalic acid, (H₂tfBDC), forms nine novel crystals with a series of N-containing heterocycles : 2,3-dimethyl pyrazine (2,3-Pyr), 2,6-dimethyl pyrazine (2,6-Pyr), 2,4-diamino-6-methyl-1,3,5-triazine (dmt), Benzoguanamine (bga), 2-methylbenzimidazole (2-MeBzImH), 1,4-bis(imidazol) butane (bimb), 2-amino-4-hydroxy-6-methyl pyrimidine (ahmp), 1,2-bis[(2-methylimidazol-1-yl)methyl] benzene (L7), and 1,4-bis[(2-methylimidazol-1-yl)methyl] benzene (L5). These crystal structures including salts/co-crystals/hydrates were analyzed and characterized by single crystal X-ray diffraction, IR, and TGA. Single crystal X-ray diffraction studies show that the huge numbers of hydrogen bonds play a significance part in assembling individual molecules into larger architectures, especially, the strong N-H \cdots O, O-H \cdots O hydrogen bonds, and weak but highly directional C-H \cdots O and C-H \cdots F interactions exist commonly in all nine novel crystals. Crystal structures analysis show that the F atom of the H₂tfBDC participates in C-H \cdots F hydrogen bond formation, producing different supramolecular synthons. More importantly, the N-H \cdots O, O-H \cdots O, and C-H \cdots O hydrogen bonds mainly involve in supramolecular assembling of these molecules, but C-H \cdots F hydrogen bonds expend two-dimensional networks into three dimensional, hence, the C-H \cdots F interactions having a crucial role in the formation of higher-order supramolecular structures.

Introduction

Considerable efforts have been devoted to noncovalent weak intermolecular interactions including hydrogen bonds, π - π stacking, and van der Waals forces etc, for their unquestionable role in designing the novel materials.¹ The intermolecular interactions have been established as the simplest possible and the most efficient tool for constructing predictable structure from different discrete molecular.^{2,3} Among these interactions, the hydrogen bonds have caused widespread concern on account of their energy and directionality.⁴ Also, the hydrogen bonds are robust in nature and retain their geometrical features over a variety of compounds.⁵ When it comes to the hydrogen bonds, it is worth to say O-H \cdots O, O-H \cdots N,

N-H \cdots O, N-H \cdots N, and the weak interactions C-H \cdots O, C-H \cdots F. However, their influence on molecular recognition is still a challenge basing on experimental and theoretical techniques.⁶

In the last decade, the halogen bonds are drawing more and more attentions as the development of the crystal engineering, analogous to hydrogen bond and it can be used as an alternative to the hydrogen bond,⁷ because the halogen atom plays an equivalent role to that of the hydrogen atom in the hydrogen bond. So, halogenated compounds, especially, fluorinated molecules, owing to its dramatic influence on the organic molecular have obtained considerable attention in chemistry, biology and the life science.⁸ Moreover, introduction the fluorine atom (fifteen percent of pharmaceuticals contain at least one fluorine atom⁹) into biologically active compounds can improve bioavailability, pharmacological properties, and metabolic stability. Thanks to its high electronegativity, low bond strength and polarizability.^{9a,10}

What's more, the experiment results indicate that the terephthalic acid (H₂BDC) is one of the most frequently used linker ligands for the supramolecular. By analysing the existing constructions in the

^a College of Chemistry and Molecular Engineering, Qingdao University of Science and Technology, Qingdao 266042, P. R. China. E-mail: inorchemwl@126.com; Fax: (+86) 532-840-22681

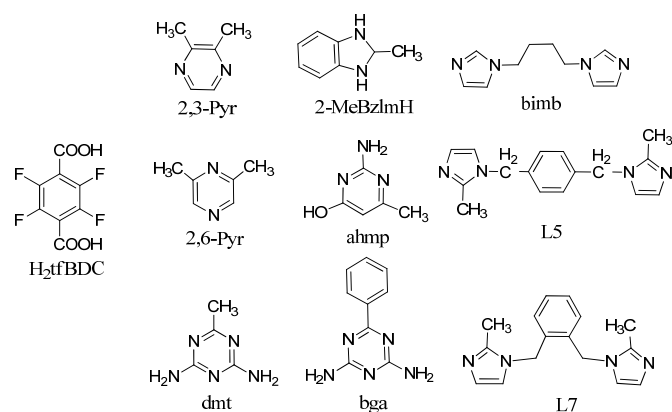
^b State Key Laboratory of Inorganic Synthesis and Preparative Chemistry, Jilin University, Changchun, 130012, PR China. E-mail: kkhuang@jlu.edu.cn;

† Electronic Supplementary Information (ESI) available: IR, TGA and DSC data. CCDC reference numbers 982115-982123. For ESI and crystallographic data in CIF or other electronic format see DOI:XXXXXXXXXX

CCDC, we discovered that from 1972 R. E. Cobblestick and R. W. H. Small synthesised a salt $\text{NH}_4^+\text{C}_6\text{H}_4\text{COOHCOO}^-$ to Selena L. Staun and Allen G. Oliver composed a hydrate $2\text{C}_5\text{H}_5\text{NO}\cdot\text{C}_8\text{H}_6\text{O}_4\cdot 2\text{H}_2\text{O}$ in 2012¹¹ approximate 1565 compounds which used H_2BDC as the linker ligand has been synthesised. Contrast with H_2BDC , utilize tetrafluoroterephthalic acid (H_2tfBDC) to assemble the multi-component molecular solids are rare. So we select the derivative of H_2BDC - H_2tfBDC as our object of study. More than that, H_2tfBDC has its unique advantages compared to non-fluorinated H_2BDC . First, significantly enhanced acidity, which is devoted to the inability of compounds to crystallize under strongly acidic atmosphere.¹² Furthermore, in fluorinated H_2tfBDC , the carboxylate groups are typically twisted out of the plane of the benzene ring and the respective torsion angles are considerably enlarged ($45\text{--}60^\circ$). This might be attributed to the high electrostatic repulsion between the fluorine atoms on the ring and the oxygen atoms of the carboxylate groups as well as a decrease in aromatic character of the carboxylate group due to the electron-withdrawing nature of the fluorine atoms.¹²

Our interest is absorbed in the interactions $\text{C-H}\cdots\text{F}$, which the F-based intermolecular interactions are considered weak, and the C-F bond has the poor hydrogen bond acceptor ability.¹³ Moreover, in fluorine-rich compounds the C-F bond is easier to form $\text{C-H}\cdots\text{F}$ interactions instead of $\text{F}\cdots\text{F}$ interactions, unlike the C-Cl, C-Br, and C-I groups in several studies.¹⁴ Hülliger and his co-workers and several other research groups all over the world have highlighted the role of fluorine involved interactions ($\text{C-H}\cdots\text{F}$, $\text{C-H}\cdots\pi$, $\text{F}\cdots\text{F}$).¹⁵ Although, these interactions are considered weak, while they play a vital role in directing the molecular assembly especially used for constructing three-dimensional (3D) network.¹⁶

Lately, we have reported an article about the H_2tfBDC with the 3-hydroxypyridine, 2-aminopyrimidine, 4-dimethylaminopyridine, 4,4'-bipyridine, 2,5-bis(4-pyridyl)-1,3,4-oxadiazole, o-phenanthroline, and imidazole-eight novel compounds,¹⁷ in order to make it more systematic, we synthesised another nine crystals in this article and the structural analysis of these crystals will be come into view. (Scheme 1)



Scheme 1 Molecular structure of H_2tfBDC and coformers discussed in this study : 2,3-Pyr, 2,6-Pyr, dmt, 2-MeBzImH, ahmp, bga, bimb, L5, L7.

Experimental section

General materials and methods

All reagents, chemicals, and solvents were purchased from commercial sources and used without any further purification. The ligand 1,4-bis(imidazol-2-yl)butane (bimb), 1,2-bis[(2-methylimidazol-1-yl)methyl]benzene (L7), and 1,4-bis[(2-methylimidazol-1-yl)methyl]benzene (L5), which were prepared according to the previously published literature procedures.¹⁸⁻¹⁹ Melting point measurements were carried out using a WRS-1B digital thermal apparatus without correction and refer to the temperature at the start of the melt. Carbon, hydrogen, and nitrogen contents were performed with a Perkin-Elmer 2400 elemental analyzer. IR of supramolecular samples were recorded with a Nicolet Impact 410 FTIR spectrometer and the samples were prepared as KBr pellets in range $4000\text{--}400\text{ cm}^{-1}$. Absorptions are denoted as follows: strong (s), medium (m), and weak (w) in the synthesis section. TGA experiments were taken on a Perkin-Elmer TGA 7 thermogravimetric analyzer from 0 to 900°C under nitrogen atmosphere at a heating rate of $10^\circ\text{C}/\text{min}$. The nine novel crystals were composed as follows.

Syntheses of the complexes 1-9

Synthesis of $[(\text{C}_6\text{H}_8\text{N}_2)\cdot(\text{C}_8\text{H}_2\text{F}_4\text{O}_4)]$ Cocrystal, (1) A solution of 2,3-dimethyl pyrazine (22 μL , 0.10 mmol) in 5 mL of methanol was mixed with H_2tfBDC (23.8 mg 0.10 mmol) in 5 mL distilled water. The reaction mixture was stirred for 15 min and obtained a clear homogeneous solution. Then the solution was allowed to stand at room temperature for slow evaporation. Colorless, block crystals were gained after two weeks. The obtained crystals were separated from the mother solution by filtration, washed with methanol-distilled water solution ($v/v = 1:1$), and dried under vacuum. Yield: 76%, m.p. : 190°C . Anal. calcd for $\text{C}_{14}\text{H}_{10}\text{F}_4\text{N}_2\text{O}_4$: C, 48.55; H, 2.89; N, 8.09%. Found: C, 48.92; H, 2.97; N, 8.11%. Infrared spectrum (KBr disc, cm^{-1}): 3434w, 3097w, 3014w, 2931w, 2796w, 2448m, 1728s, 1654m, 1484s, 1432m, 1407s, 1385s, 1317s, 1214s, 1179s, 1000s, 887w, 861m, 841w, 781w, 771m, 747m, 712s, 621w, 543m, 491m, 463m, 439m.

Synthesis of $[(\text{C}_6\text{H}_8\text{N}_2)\cdot(\text{C}_8\text{H}_2\text{F}_4\text{O}_4)]$ Cocrystal, (2) To an acetone-distilled water solution ($v/v = 1:1$, 10 mL) containing 2,6-dimethyl pyrazine (21.6 mg, 0.20 mmol) was added H_2tfBDC (23.8 mg, 0.10 mmol) with constant stirring for 15 min. The clear and homogeneous solution was slowly evaporated at room temperature, and block colorless crystals were obtained three weeks later. The crystals were picked up from the mother liquor and washed with acetone-distilled water solution ($v/v = 1:1$), and dried under vacuum. Yield: 70%, m.p. : 166°C . Anal. calcd for $\text{C}_{14}\text{H}_{10}\text{F}_4\text{N}_2\text{O}_4$: C, 48.55; H, 2.89; N, 8.09%. Found: C, 48.85; H, 2.87; N, 8.2%. Infrared spectrum (KBr disc, cm^{-1}): 3447m, 3083m, 2806m, 2533m, 1728s, 1642m, 1607w, 1540m, 1482s, 1406m, 1383m, 1324s, 1279s, 1248m, 1216s, 1165s, 1039m, 997s, 943m, 895m, 875m, 837w, 791w, 768m, 743m, 709s, 663w, 611m, 566m, 517m, 499m, 476m, 462m.

Synthesis of $[(\text{C}_4\text{H}_8\text{N}_5^+)_2\cdot(\text{C}_8\text{F}_4\text{O}_4^{2-})]$ Salt, (3) 2,4-diamino-6-methyl-1,3,5-triazine (12.6 mg, 0.10mmol) was dissolved in 5 mL of 1,4-dioxane followed by the addition of 5 mL distilled water solution of H_2tfBDC (23.8 mg, 0.10 mmol). The resulting colorless solution was stirred for 15 min and kept at room temperature for crystallization. Colorless block shaped crystals after three weeks in about 75% yield were filtered and washed with 1,4-dioxane - distilled water solution ($v/v = 1:1$), then dried in vacuum desiccators.

m.p. : 236°C. Anal. calcd for $C_{16}H_{16}F_4N_{10}O_4$: C, 39.34; H, 3.28; N, 28.69%. Found: C, 39.42; H, 3.36; N, 28.52%. Infrared spectrum (KBr disc, cm^{-1}): 3466s, 3346s, 2953m, 2884m, 2378w, 1656s, 1473s, 1377m, 1225m, 1165m, 1082m, 1042m, 996s, 875w, 832w, 793m, 778m, 720m, 636m, 520m.

Synthesis of $[(C_9H_{10}N_5)^2 \cdot (C_8H_2F_4O_4) \cdot (C_8F_4O_4)^2]$ Salt, (4) 5 mL acetonitrile solution of 2,4-diamino-6-phenyl-1,3,5-triazine (18.7 mg, 0.10 mmol) was mixed to 5 mL distilled water solution of H_2tfBDC (23.8 mg, 0.10 mmol), and the colorless solution was stirred for 15 min and kept for slow evaporation at room temperature. Colorless block shaped crystals in about 80% yield were obtained after three weeks and separated from the mother liquor. Washed the crystals with the acetonitrile-distilled water solution ($v/v = 1:1$) and dried under vacuum. m.p. : 246°C. Anal. calcd for $C_{34}H_{22}F_8N_{10}O_8$: C, 47.94; H, 2.59; N, 16.45%. Found: C, 47.88; H, 2.64; N, 16.48%. Infrared spectrum (KBr disc, cm^{-1}): 3403s, 2389m, 1972m, 1695s, 1625s, 1483s, 1357s, 1299s, 1220m, 1192m, 1161m, 1055m, 984s, 935w, 898w, 879w, 848w, 809m, 790m, 776s, 733s, 682m, 662m, 612m, 598m, 566m, 485m, 464m.

Synthesis of $[C_8H_9N_2]^+ \cdot (C_8HF_4O_4)_3]$ Salt, (5) A solution of H_2tfBDC (23.8 mg, 0.10 mmol) was prepared in 5 mL of distilled water. 5 mL 1,4-dioxane solution of 2-methyl benzimidazole (13.2 mg, 0.10 mmol) was added to the above solution. The resulting solution was stirred for 15 min and kept at room temperature for crystallization. Colorless, block crystals were gained after two weeks. The obtained crystals were separated from the mother solution by filtration, washed with 1,4-dioxane-distilled water solution ($v/v = 1:1$), and dried under vacuum. Yield: 78%, m.p. : 218°C. Anal. calcd for $C_{48}H_{29}F_{12}N_6O_{12}$: C, 51.89; H, 2.61; N, 7.57%. Found: C, 51.92; H, 2.66; N, 7.68%. Infrared spectrum (KBr disc, cm^{-1}): 3072s, 2477m, 2389m, 2106w, 1938w, 1721s, 1626s, 1569m, 1513m, 1461s, 1419m, 1364s, 1270m, 1227m, 1200m, 1159m, 1124m, 1029s, 997s, 962m, 892m, 848s, 802m, 757s, 711s, 624m, 512m, 472m, 456m.

Synthesis of $[(C_{10}H_{16}N_4)^{2+}]_{0.5} \cdot (C_8HF_4O_4)_2]$ Salt, (6) H_2tfBDC (23.8 mg, 0.10 mmol) and 1,4-bis(imidazol) butane (9.5 mg, 0.05 mmol) were taken in a 2:1 molar ratio and dissolved in ethanol-distilled water solution ($v/v = 1:1$ 10 mL), the solution was stirred for 15 min until obtained the colorless solution. Good quality crystals, suitable for diffraction, were gained after one week as the solution slow evaporation at room temperature. The obtained crystals were picked up from the mother liquor by filtration, use the ethanol - distilled water solution ($v/v = 1:1$) to wash, and dried in vacuum desiccators. Yield: 82%, m.p. : 176°C. Anal. calcd for $C_{13}H_9F_4N_2O_4$: C, 46.85; H, 2.70; N, 8.41%. Found: C, 46.88; H, 2.64; N, 8.45%. Infrared spectrum (KBr disc, cm^{-1}): 3435w, 3177m, 3144m, 3072m, 2944m, 2821m, 2741m, 1701s, 1574m, 1549m, 1469s, 1407m, 1367m, 1302s, 1249m, 1087m, 1034m, 993s, 898m, 875m, 837m, 793m, 764m, 741m, 715s, 627m, 570w, 511m, 498m, 466m, 440w.

Synthesis of $[(C_5H_8N_3O)^+ \cdot (C_8F_4O_4)^{2-}]_{0.5} \cdot (C_8H_2F_4O_4)_{0.5} \cdot H_2O]$ Hydrate, (7) H_2tfBDC (23.8 mg, 0.10 mmol) and 2-amino-4-hydroxy-6-methyl pyrimidine (12.5 mg, 0.10 mmol) were dissolved in 10 mL 1,4-dioxane-distilled water mixed solvent and stirred until the solids disappeared and formed the colorless solution. The

solution was kept for crystallization at room temperature. Colorless blocks of crystals crystallized from solution after two weeks. The obtained crystals were separated from the mother liquor by filtration, washed with 1,4-dioxane-distilled water mixed solvent ($v/v = 1:1$), and dried in vacuum. Yield: 74%, m.p. : 295°C. Anal. calcd for $C_{26}H_{22}F_8N_6O_{12}$: C, 40.89; H, 2.88; N, 11.01%. Found: C, 39.42; H, 2.84; N, 11.20%. Infrared spectrum (KBr disc, cm^{-1}): 3361m, 2932m, 1698s, 1494m, 1469m, 1426m, 1391m, 1364m, 1274w, 1246w, 1182w, 1384s, 1144w, 1076w, 1041w, 988m, 941w, 839m, 787m, 733m, 647m, 592m, 555m, 502m.

Synthesis of $[(C_{16}H_{20}N_4)^2 \cdot (C_8HF_4O_4)_2 \cdot 2H_2O]$ Hydrate, (8) 1,2-bis[(2-methylimidazol-1-yl)methyl] benzene (15.1 mg, 0.05 mmol) was dissolved in 5 mL of ethanol, and H_2tfBDC (23.8 mg, 0.10 mmol) was dissolved in 5 mL of distilled water. Both the solutions were mixed and stirred at room temperature. About 15 min later got the homogeneous solution and allowed to stand at room temperature for slow evaporation. Three weeks later crystals started coming out and the yield about 73%. It was further stirred and washed with ethanol-distilled water ($v/v = 1:1$), and dried in vacuum desiccators. m.p. : 174°C. Anal. calcd for $C_{32}H_{24}F_8N_4O_9$: C, 50.46; H, 3.15; N, 7.36%. Found: C, 50.45; H, 3.25; N, 7.52%. Infrared spectrum (KBr disc, cm^{-1}): 3392m, 3162m, 3110m, 2985w, 2904w, 2660m, 2472m, 1730m, 1623m, 1600m, 1533m, 1471s, 1431m, 1390m, 1367m, 1296m, 1150m, 1213m, 1106m, 1048m, 992s, 946m, 918m, 872m, 853m, 839w, 786m, 768m, 737m, 708s, 656m, 640w, 618w, 585w, 510w, 483w.

Synthesis of $[(C_{16}H_{20}N_4)^2 \cdot (C_8HF_4O_4)_2]$ Salt, (9) 15.1 mg of 1,4-bis[(2-methylimidazol-1-yl) methyl] benzene (0.05 mmol) was dissolved in 5 mL of ethanol and 5 mL distilled water of H_2tfBDC (23.8 mg, 0.10 mmol) was added to this solution and stirred for 15 min to get a homogeneous solution. The resultant solution was allowed to evaporate slowly at room temperature, colorless block-like crystals suitable for X-ray diffraction were obtained in about 76% yield within two weeks. The crystals were separated from the mother liquor by filtration, washed with ethanol-distilled water solution ($v/v = 1:1$), and dried under vacuum, m.p. : 182°C. Anal. calcd for $C_{32}H_{20}F_8N_4O_8$: C, 51.82; H, 2.71; N, 7.56%. Found: C, 51.90; H, 2.77; N, 7.52%. Infrared spectrum (KBr disc, cm^{-1}): 3433w, 3167m, 3147m, 3078w, 2982m, 2916m, 2642m, 1894m, 1716m, 1616m, 1531m, 1480s, 1432m, 1380s, 1309s, 1279s, 1232m, 1211m, 1146m, 1119m, 1045m, 991s, 920m, 887m, 872m, 851w, 773m, 760m, 743m, 729s, 712s, 655m, 515m, 492m, 462m.

X-Ray crystallography

The sample for single crystal diffraction of compounds 1-9 were synthesised through the manner described above and selected to glue at the top of a thin glass fiber with epoxy glue in air for data collection, and the crystallographic data were collected on a Siemens Smart CCD diffractometer equipped with a normal-focus, 2.4-kW sealed-tube X-ray source (graphite-monochromatic MoK α radiation ($\lambda = 0.71073 \text{ \AA}$)) operating at 50 kV and 40 mA. The crystal structures were solved by direct method and refined on F^2 by full-matrix leastsquares methods using the SHELXL²⁰ program package. The crystal data are presented in Table 1.

Table 1 Crystal data and structure refinement summary for compounds **1-9**

	1	2	3	4	5	6
Empirical formula	C ₁₄ H ₁₀ F ₄ N ₂ O ₄	C ₁₄ H ₁₀ F ₄ N ₂ O ₄	C ₁₆ H ₁₆ F ₄ N ₁₀ O ₄	C ₃₄ H ₂₂ F ₈ N ₁₀ O ₈	C ₄₈ H ₃₀ F ₁₂ N ₆ O ₁₂	C ₁₃ H ₉ F ₄ N ₂ O ₄
Formula wt	346.24	346.24	488.39	850.62	1110.78	333.22
Crystal system	Triclinic	Triclinic	Monoclinic	Triclinic	Monoclinic	Triclinic
Space group	<i>P</i> $\bar{1}$	<i>P</i> $\bar{1}$	<i>P</i> 2(1)/ <i>n</i>	<i>P</i> $\bar{1}$	<i>C</i> 2/ <i>c</i>	<i>P</i> $\bar{1}$
<i>a</i> /Å	8.1577(6)	7.8250(4)	4.8860(12)	7.6570(4)	28.889(2)	7.3027(6)
<i>b</i> /Å	10.1407(8)	9.0424(4)	11.475(3)	10.0492(8)	9.7001(8)	9.6227(7)
<i>c</i> /Å	18.2913(14)	11.6340(4)	17.771(4)	11.3387(4)	19.7288(16)	9.7417(7)
α /°	95.2070(10)	92.810(3)	90	89.108(4)	90	94.022(6)
β /°	94.8800(10)	105.233(4)	90.010(10)	86.461(3)	129.1980(10)	109.536(7)
γ /°	98.6630(10)	115.272(5)	90	83.070(5)	90	90.479(6)
<i>V</i> /Å ³	1482.2(2)	705.88(5)	996.3(4)	864.42(9)	4284.4(6)	643.20(8)
<i>Z</i>	4	2	2	1	4	2
<i>D</i> _{calcd} /g cm ⁻³	1.552	1.629	1.628	1.634	1.722	1.721
μ /mm ⁻¹	0.146	0.154	0.146	0.147	0.158	0.165
T/K	293	293	293	293	293	293
<i>F</i> (000)	704	352	500	432	2256	338
Total/Independent reflections	9552/6797	5580/3339	6184/2405	6912/4007	13375/5219	4750/2956
Data/Restraints/Parameters	6797/0/433	3339/0/217	2405/0/154	4007/0/271	5219/0/353	2956/0/208
<i>R</i> _{int}	0.0706	0.0189	0.0429	0.0190	0.0471	0.0165
Final <i>R</i> ₁	0.0770	0.0959	0.0530	0.0680	0.1089	0.0635
w <i>R</i> ₂ [all data]	0.1823	0.1871	0.1446	0.1367	0.1912	0.1181
GOF on <i>F</i> ²	1.070	1.034	1.083	1.042	0.909	1.054

	7	8	9
Empirical formula	C ₁₃ H ₁₁ F ₄ N ₃ O ₆	C ₃₂ H ₂₄ F ₈ N ₄ O ₉	C ₃₂ H ₂₂ F ₈ N ₄ O ₈
Formula wt	381.25	760.55	742.54
Crystal system	Monoclinic	Monoclinic	Triclinic
Space group	<i>P</i> 2(1)/ <i>n</i>	<i>P</i> 2(1)/ <i>c</i>	<i>P</i> $\bar{1}$
<i>a</i> /Å	6.1044(4)	9.0755(4)	7.1153(5)
<i>b</i> /Å	12.0203(6)	36.884(2)	8.4148(6)
<i>c</i> /Å	20.6007(13)	9.7005(3)	14.4196(13)
α /°	90	90	99.8950(10)
β /°	97.195(5)	93.508(3)	97.073(2)
γ /°	90	90	111.8780(10)
<i>V</i> /Å ³	1499.71(16)	3241.0(3)	772.54(10)
<i>Z</i>	4	4	1
<i>D</i> _{calcd} /g cm ⁻³	1.689	1.559	1.596
μ /mm ⁻¹	0.164	0.144	0.147
T/K	293	293	293
<i>F</i> (000)	776	1552	378
Total/Independent reflections	7007/3515	19041/7709	4968/3540
Data/Restraints/Parameters	3515/0/240	7709/3/486	3540/0/235
<i>R</i> _{int}	0.0365	0.0308	0.0351
Final <i>R</i> ₁	0.1075	0.0932	0.0644
w <i>R</i> ₂ [all data]	0.1035	0.1276	0.1597
GOF on <i>F</i> ²	0.999	1.024	1.083

Crystallization of tetrafluoroterephthalic acid with 2,3-dimethyl pyrazine (1:1), 2,6-dimethyl pyrazine (1:2), 2,4-diamino-6-methyl-1,3,5-triazine (1:1), 2,4-diamino-6-phenyl-1,3,5-triazine (1:1), 2-methyl benzimidazole (1:1), 1,4-bis(imidazol) butane (2:1), 2-amino-4-hydroxy-6-methyl pyrimidine (1:1), 1,2-bis[(2-methylimidazol-1-yl)methyl] benzene (2:1), 1,4-bis[(2-methylimidazol-1-yl)methyl] benzene (2:1) results in crystals. Both base-type and acid-type reagents have good solubility in distilled water and some common organic solvents, for instance, methanol, ethanol, acetone, 1,4-dioxane, and acetonitrile. The crystal structures of all nine materials (**1-9**) were carried out in different ratios and different solvents. Nine new solid forms were obtained from different solvent combinations: two cocrystals: with 2,3-dimethyl pyrazine (1) and 2,6-dimethyl pyrazine (2); two hydrous salts: with 2-amino-4-hydroxy-6-methyl pyrimidine (7) 1,2-bis[(2-methylimidazol-1-yl)methyl] benzene (8); five salts: 2,4-diamino-6-methyl-1,3,5-triazine (3), 2,4-diamino-6-phenyl-1,3,5-triazine (4), 2-methyl benzimidazole (5), 1,4-bis(imidazol) butane (6), 1,4-bis[(2-methylimidazol-1-yl)methyl] benzene (9). However, they exhibit many common features, especially in the formation of hydrogen bonds. Be just like most of the supramoleculars, these crystals contain a great deal of hydrogen bond networks in which the tetrafluoroterephthalic acid and base components form a series of possible synthons. The schematic representations of different kinds of hydrogen-bonding synthons related to this work are summarized in **Scheme 2**. The crystallographic parameters is summarized in **Table 1**. Hydrogen-bond geometries of **1-9** are listed in **Table 2**. Now we discuss the structural aspects of these new multi-component crystals.

Results and discussion

Preparation of compounds **1-9**

In our initial crystallizations, we varied the stoichiometries of tetrafluoroterephthalic acid and base-type reagents (1:2, 1:1, and 1:2) in parallel solution experiments. However, for this three different ratios, we obtained nine novel crystals.

Table 2 Characteristics of hydrogen-bond geometries observed in the crystal structures of **1-9**

D-H...A (Å)	D-H(Å)	H...A(Å)	D...A(Å)	D-H...A (deg)
1 O2-H2...N1 ^a	0.82	1.83	2.643	173.0
O8-H8...N2 ^a	0.82	1.88	2.669	161.4
O5-H5...N3 ^b	0.82	1.83	2.643	176.3
O4-H4...N4 ^b	0.82	1.87	2.669	164.5
C17-H17C...O1 ^d	0.96	2.62	3.551	146.1
C12-H12C...F1 ^c	0.96	2.70	3.537	126.6
2 C6-H6B...O2 ^e	0.96	2.64	3.500	149.1
C6-H6A...F4 ^o	0.96	2.76	3.323	118.0
C13-H13...O3 ^o	0.93	2.51	3.429	170.6
O2-H2...N2 ^f	0.82	1.93	2.739	167.7
C11-H11...O4 ^o	0.93	2.44	3.108	128.3
O1-H1...N1 ^f	0.82	1.90	2.682	159.2
3 N5-H5A...O2 ^g	0.86	2.28	3.006	175.7
N4-H4B...N1 ^h	0.86	2.15	3.006	170.3
N5-H5A...F1 ^h	0.86	2.31	3.044	164.5
N2-H2...O2 ^h	0.86	1.78	2.640	155.5
N5-H5B...O1 ^h	0.86	2.00	2.831	138.8
N4-H4A...N1 ^h	0.86	2.15	3.006	110.4
4 O1-H1...O2 ^g	0.82	1.73	2.489	154.0
N1-H1B...O2 ^g	0.86	2.10	2.820	140.5
N1-H1A...O3 ^g	0.86	2.10	2.932	161.7
C4-H4...F1 ^e	0.93	2.53	3.108	120.8
5 O5-H5...O6 ⁱ	0.82	1.77	2.482	175.3
N2-H2...O2 ⁱ	0.86	2.31	2.718	146.6
C8-H8...F6 ⁱ	0.93	2.45	3.087	140.1
N3-H3...O3 ⁱ	0.86	2.60	2.776	126.1
C5-H5A...F4 ⁱ	0.96	2.69	3.116	153.7
C9-H9...F3 ⁱ	0.93	2.73	3.300	155.1
6 O4-H4...O1 ^j	0.82	1.69	2.503	169.6
C9-H9...F1 ^k	0.93	2.50	3.315	145.7
C13-H13B...F2 ^k	0.97	2.54	3.147	120.8
C11-H11...O1 ^j	0.93	2.34	3.251	165.6
C13-H13B...F3 ^j	0.97	2.67	3.422	134.2
C10-H10...O2 ^j	0.93	1.85	2.677	146.8
N1-H1...O2 ^j	0.86	1.92	2.677	148.1
7 O4-H4...O6 ^l	0.82	1.72	2.540	173.9
O6W-H6WA...O2 ^c	0.85	1.88	2.718	164.5
N3-H3A...O2 ^c	0.86	1.91	2.752	167.9
N2-H2...O1 ^c	0.86	1.93	2.775	165.7
C26-H26B...F4 ^m	0.96	2.58	3.301	132.4
8 O4-H4...O1 ⁿ	0.82	1.69	2.503	169.7
N1-H1...O1 ⁿ	0.86	2.25	2.850	127.4
C21-H21...F8 ⁿ	0.93	2.41	3.189	141.2
N4-H4...O1We ^b	0.86	1.83	2.678	168.9
O1W-H1WA...O8 ⁿ	0.81	2.13	2.922	166.8
C10-H10...F7 ⁿ	0.93	2.45	3.292	150.8
9 N1-H1...O1 ^d	0.86	1.88	2.735	171.7
C16-H16...O1 ^d	0.93	2.46	3.303	150.7
C11-H11B...O2 ^d	0.97	2.53	3.338	140.4
C15-H15...O3 ^e	0.93	2.58	3.382	145.0
C11-H11A...O3 ^e	0.97	2.64	3.593	167.9

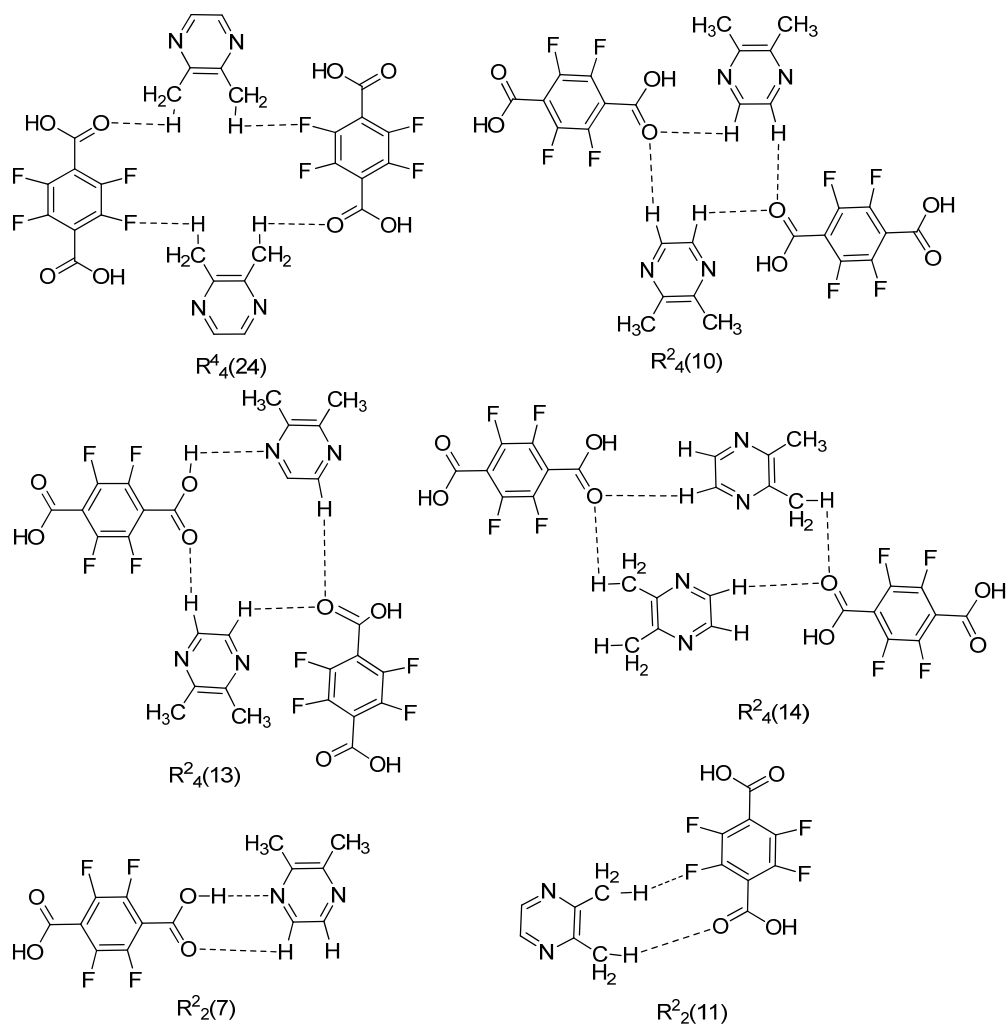
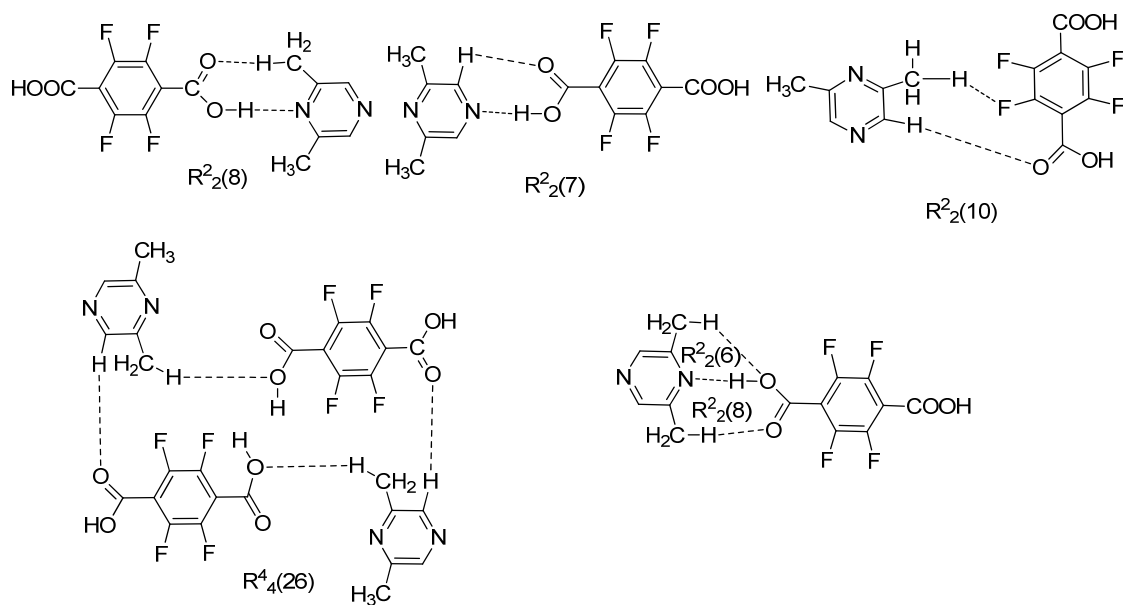
^a $1+x, 1+y, 1+z$. ^b $1+x, 1+y, z$. ^c x, y, z . ^d $1+x, y, z$. ^e $-x, 1-y, -z$. ^f $1-x, 1-y, -z$. ^g $0.5+x, -0.5+y, 0.5-z$. ^h $0.5-x, -0.5+y, 0.5-z$. ⁱ $2+x, -y, -0.5+z$. ^j $1-x, 2-y, 1-z$. ^k $3-x, -y, 3-z$. ^l $1-x, 1-y, -1-z$. ^m $1-x, 1-y, 1-z$. ⁿ $-1-x, 1-y, -1+z$. ^o $-x, -y, 1-z$.

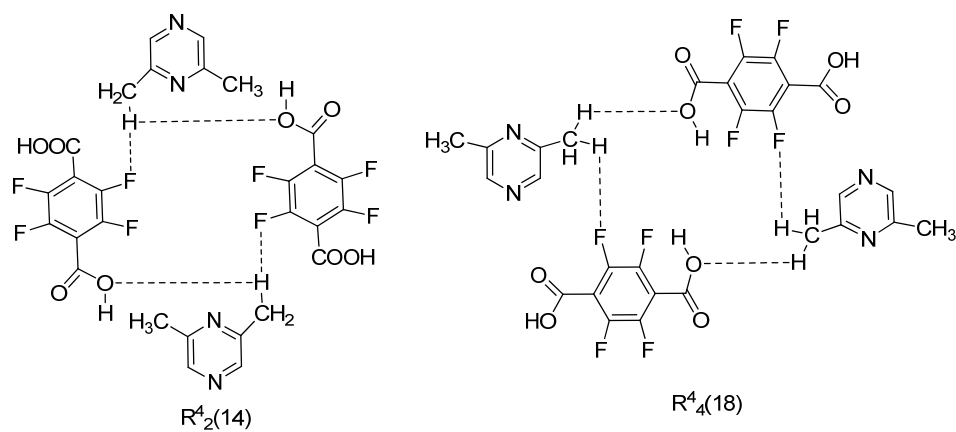
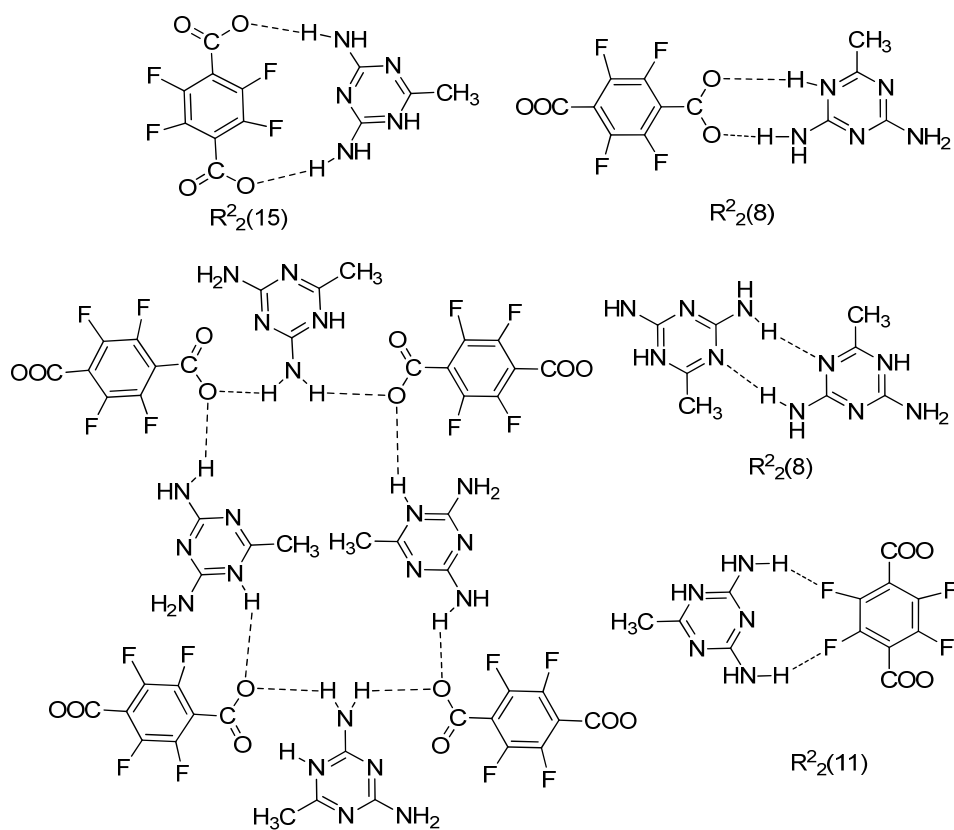
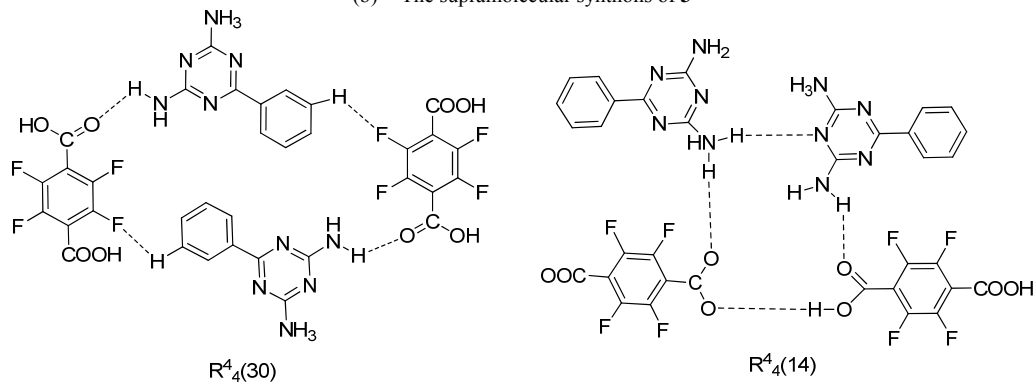
Tetrafluoroterephthalic acid/2,3-dimethyl pyrazine (1:1), (H₂tfBDC/2,3-Pyr) The crystal of compound **1** crystallizes in the triclinic system *P*1 space group (*Z*=4), and the asymmetric unit includes two molecules of H₂tfBDC and two molecules of 2,3-Pyr (Fig. 1a). The C-O/C=O bond distance of the two carboxyl groups are 1.272/1.187Å and 1.300/1.206Å, respectively. The exocyclic bond length C8-C13, C16-C20, C24-C27 and C22-C28 are elongated to 1.512, 1.508, 1.516 and 1.507Å, respectively, longer than the cyclic those of C-C bonds which length are average 1.381Å. The length of the cyclic bonds C-N are average 1.328Å, the bonds length of C-F are average 1.377Å. In this structure, the carboxylic groups of H₂tfBDC appear torsion. The dihedral angle of the two carboxylic group is 17.464(2)°, and the angles between the carboxylic groups and the benzene ring of H₂tfBDC are 67.934(1)° and 50.559(1)°, respectively.

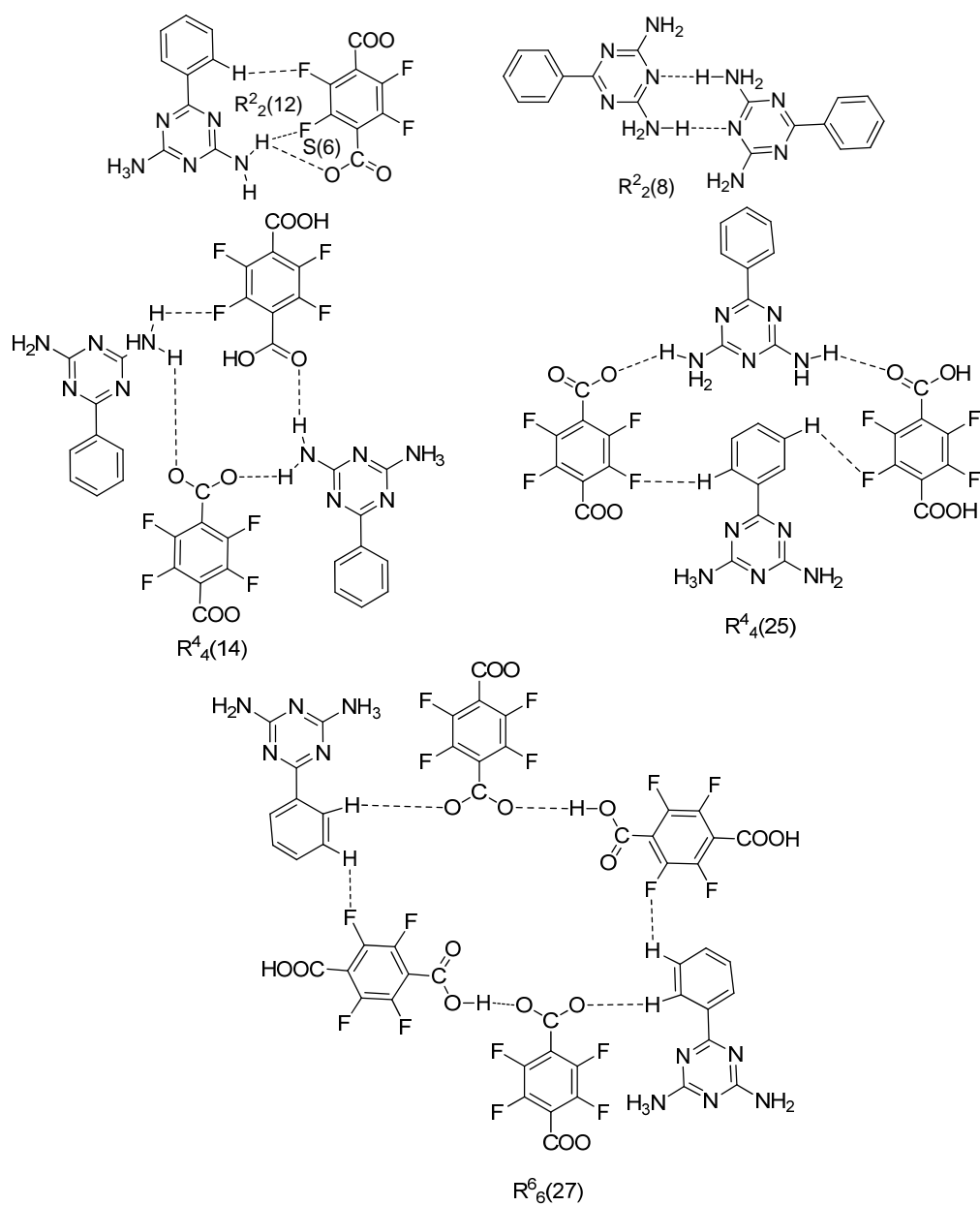
In this architecture, the H₂tfBDC and 2,3-Pyr alternate linked through the hydrogen bond of O-H...N (O5-H5...N3, 1.825Å; O2-H2...N1, 1.827Å; O3-H4...N4, 1.874Å; O8-H8...N2, 1.879Å) and formed a twisted one-dimensional chains which is shown in Figure 1b. In this chain we can find that the H₂tfBDC molecule and the 2,3-Pyr molecule via O-H...N and N-H...O hydrogen bonds formed a dimer which is emerged a hydrogen-bonded ring of R₂²(7). The adjacent chains via C-H...O weak hydrogen bonds (C17-H17C...O1, 2.617Å) generate a two-dimensional sheet. Furthermore, there are C12-H12...F1, C11-H11...O7, and C12-H12A...F8 weak hydrogen bonds link adjoining sheets to get a three-dimensional network motif (Fig. 1d). In addition, in compound **1**, synthons R₄⁴(24), R₂⁴(10), R₂²(11), R₂⁴(14), R₂²(7), and R₂⁴(13) are formed properly and shown in Scheme 2

Tetrafluoroterephthalic acid/2,6-dimethyl pyrazine (1:2), (H₂tfBDC/2,6-Pyr) Single crystals of compound **2** crystallizes have the same space group of triclinic system (*Z*=2) with crystal **1**. The asymmetric unit of compound **2** consists of one molecule of H₂tfBDC and one molecule of 2,6-Pyr (Fig. 2a). The distances of -COOH (C1-O1, 1.300Å, C21-O2, 1.293Å) demonstrate the nonionic acid. The exocyclic bond lengths C4-C21 and C1-C2 are elongated to 1.517 and 1.510Å, longer than the cyclic those of C-C bonds which length are average 1.380Å. The bond lengths C-N and C-F are average 1.332Å and 1.345Å, respectively. Within H₂tfBDC molecular moiety, the dihedral angle between carboxylic groups and benzene ring are 50.905(2)° and 46.299(3)°, the dihedral angle between the two carboxylic groups is 5.800(4)°.

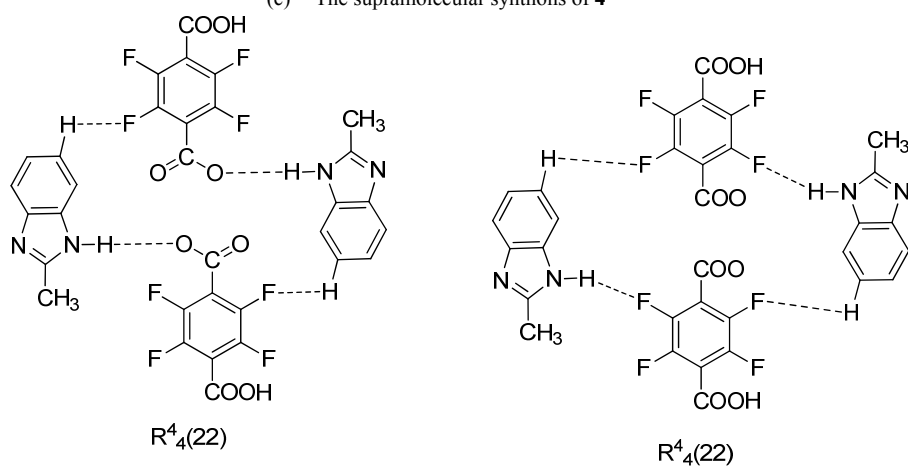
In the crystal lattice of compound **2** exist a fascinating three hydrogen bonding patterns, which is formed by the H₂tfBDC and 2,6-Pyr molecules through the O1-H1...N1 (1.899Å), C-H...O (C8-H8A...O3, 2.427Å; C6-H6A...O1, 2.413Å) hydrogen bonds, it is creating an R₂²(6) ring and an R₂²(8) ring (in Scheme 2). More than that, the other -COOH which belongs to H₂tfBDC develops a heterodimer with another 2,6-Pyr molecule via the hydrogen bonds O2-H2...N2 and C11-H11...O4. The three hydrogen bonding patterns interact with the dimers to form 1D chains. Neighboring chains are linked through C13-H13...O3 (2.509Å) interactions to form a two-dimensional layer. C-H...F hydrogen bonds play a vital part in the construction of the three-dimensional network in the Figure 2d.

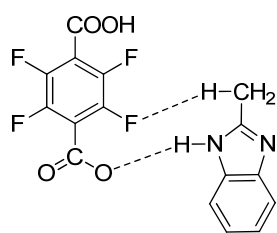
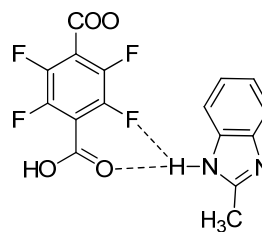
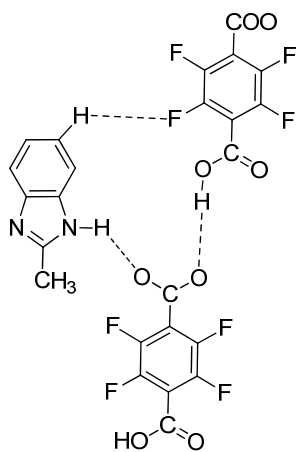
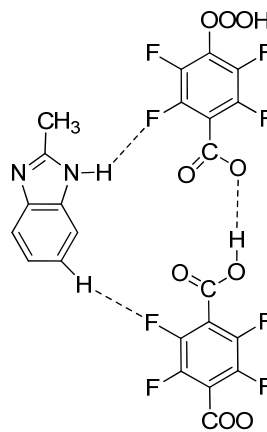
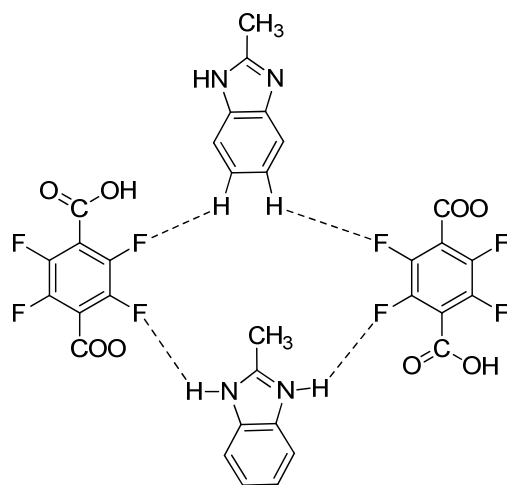
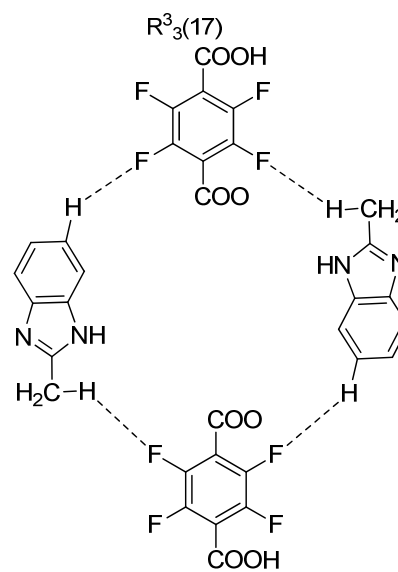
(a) The supramolecular synthons of **1**

(a) The supramolecular synthons of **2**(b) The supramolecular synthons of **3**

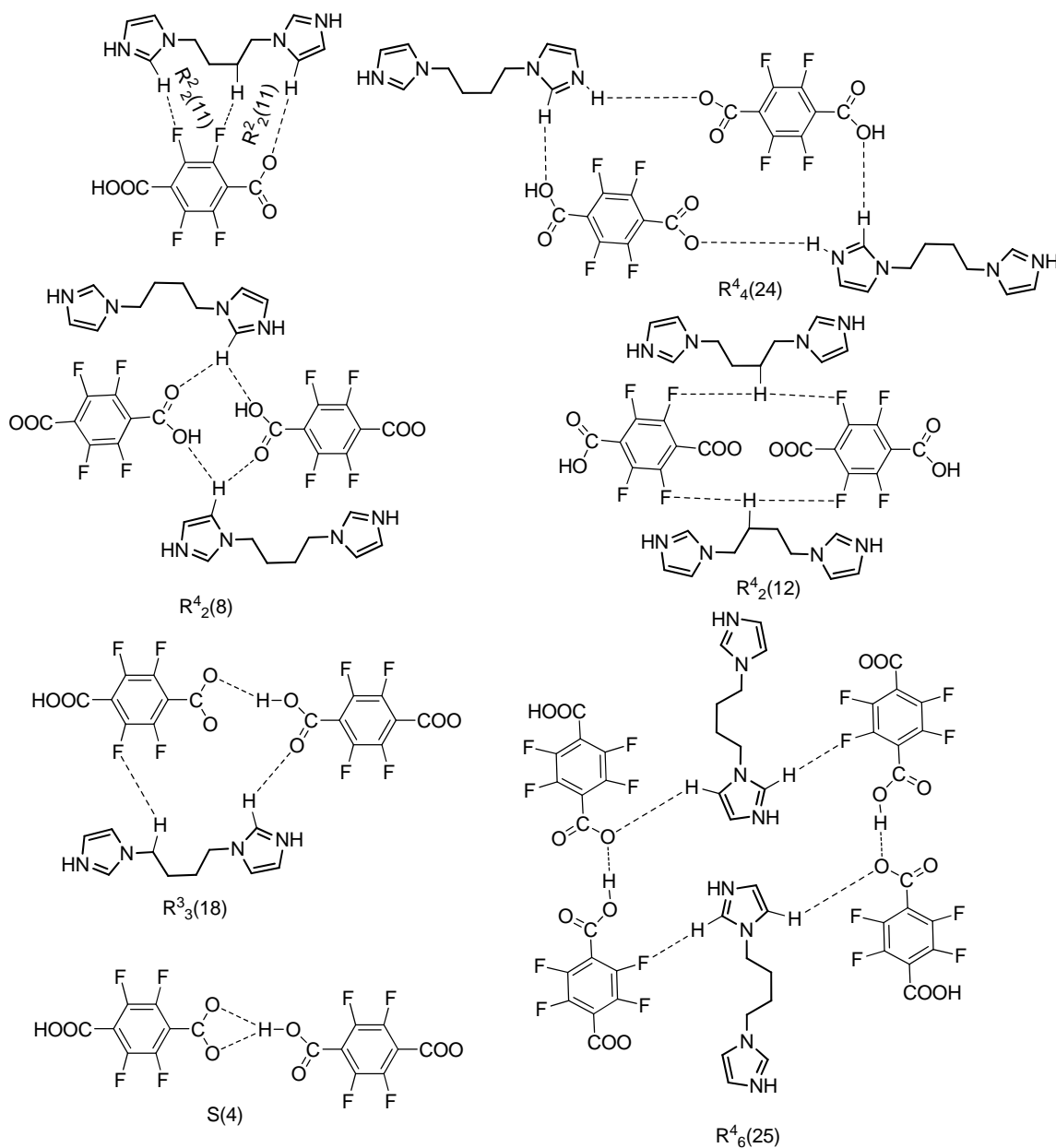


(c) The supramolecular synthons of 4

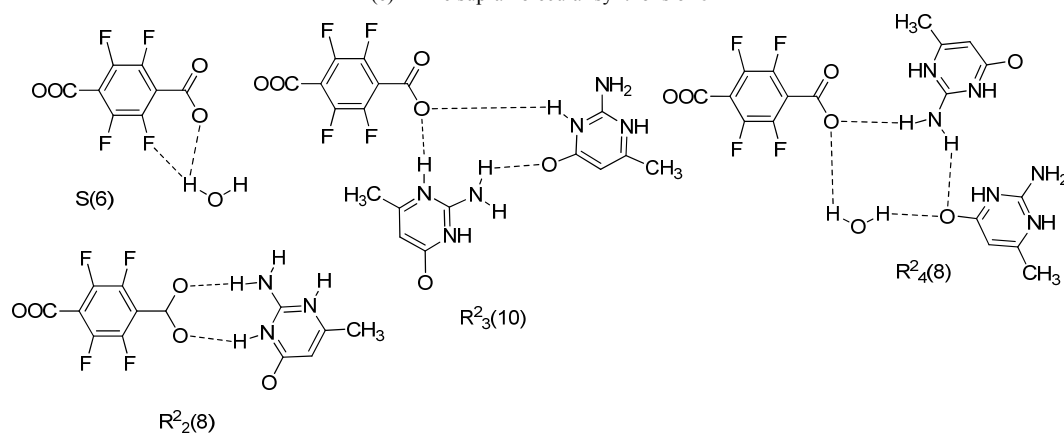


 $R^2_2(10)$  $S(6)$  $R^4_4(15)$  $R^3_3(17)$  $R^4_4(17)$  $R^4_4(26)$

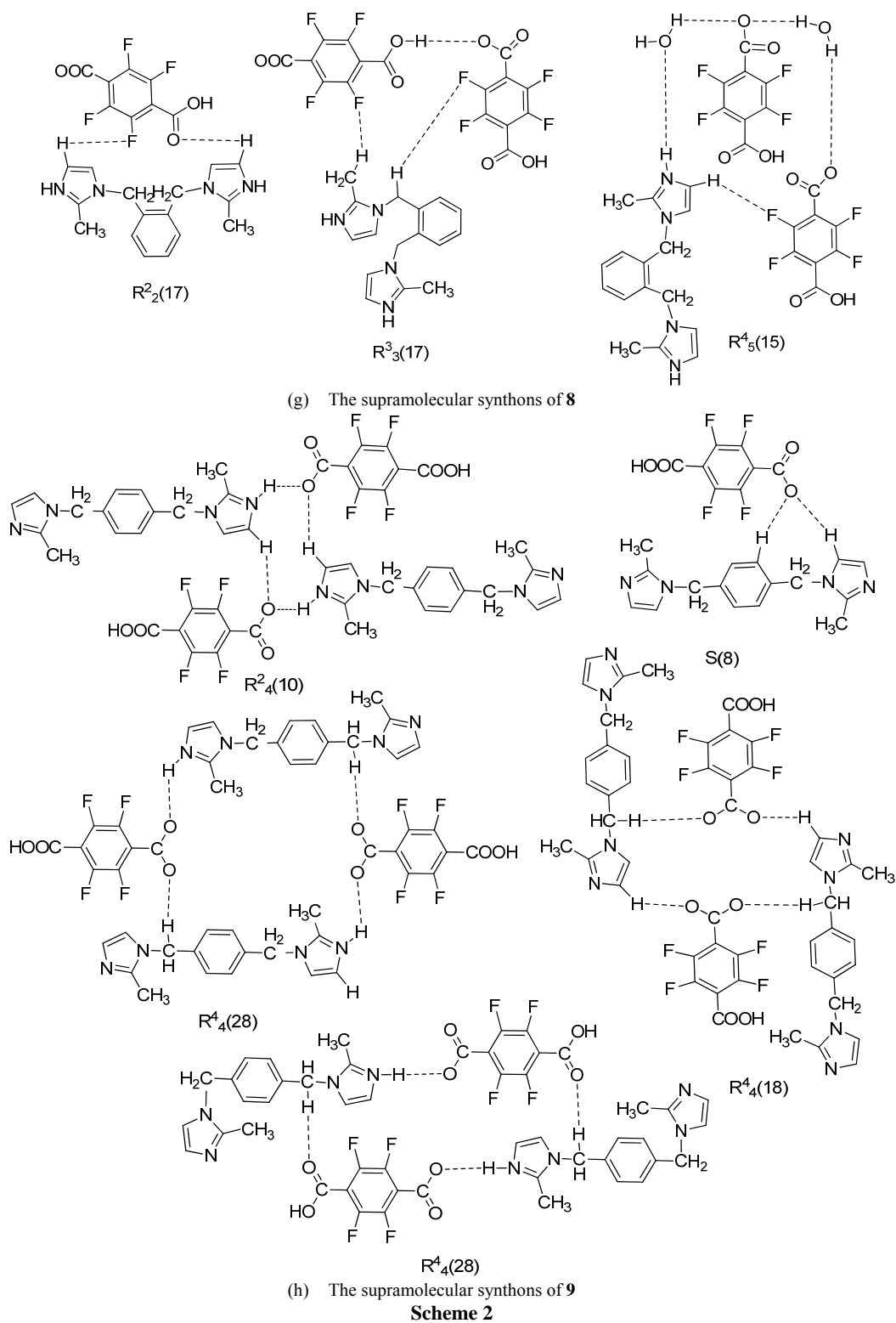
(d) The supramolecular synthons of 5



(e) The supramolecular synthons of 6



(f) The supramolecular synthons of 7



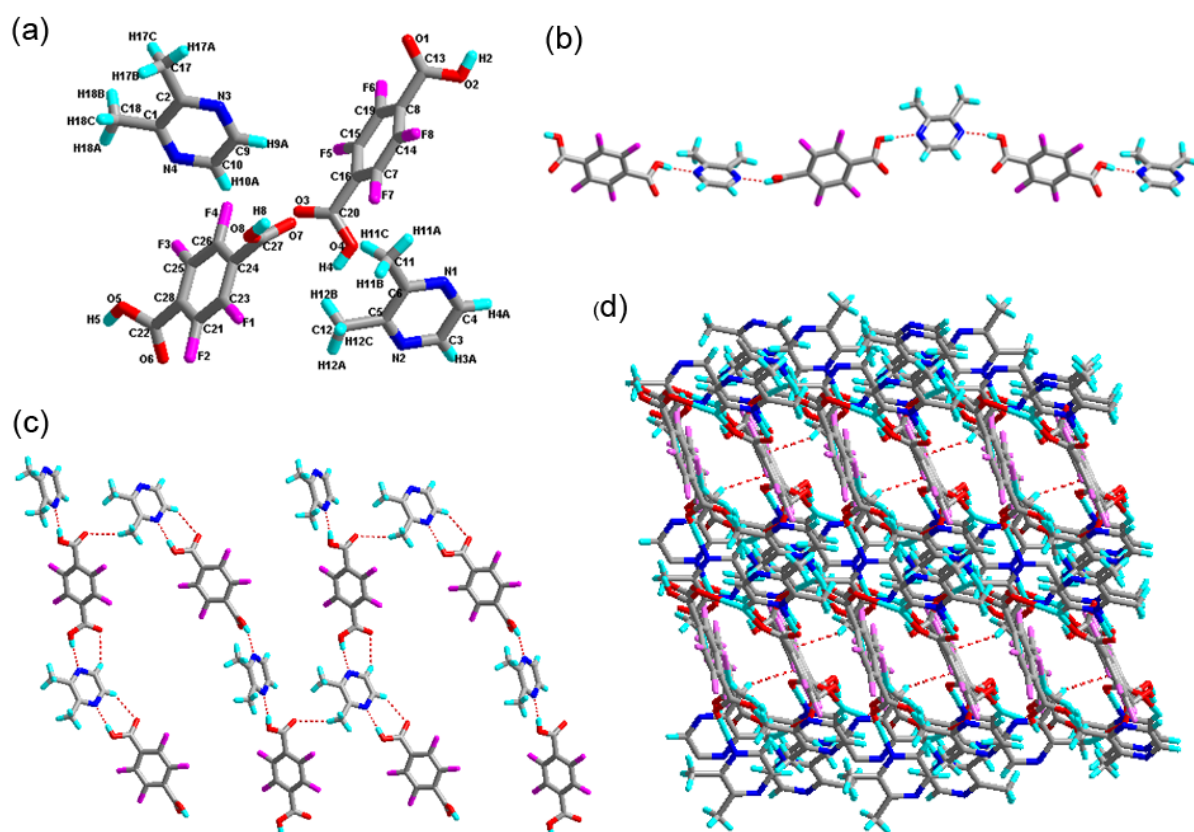


Figure 1. (a) Molecular structure of **1** with atom labeling of the asymmetric unit; (b) 1D supramolecular tape via hydrogen bonds (the hydrogen bonds are indicated as broken lines in this and the subsequent figures); (c) Perspective view of the 2D hydrogen-bonded layer; (d) the resultant 3D network. (O, red; N, blue; C, gray; H, turquoise; F, pink in this and the subsequent figures)

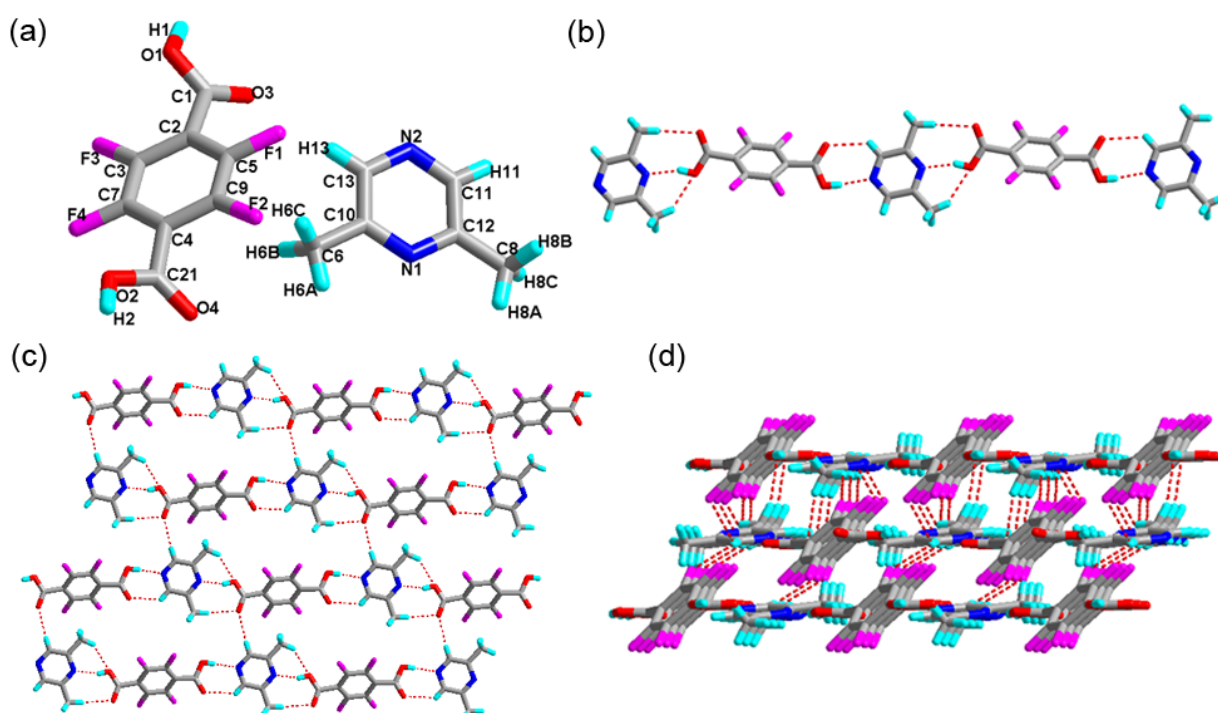


Figure 2. (a) Molecular structure of **2** with atom labeling of the asymmetric unit; (b) 1D supramolecular tape via hydrogen bonds (the hydrogen bonds are indicated as broken lines in this and the subsequent figures); (c) Perspective view of the 2D hydrogen-bonded layer; (d) the resultant 3D network

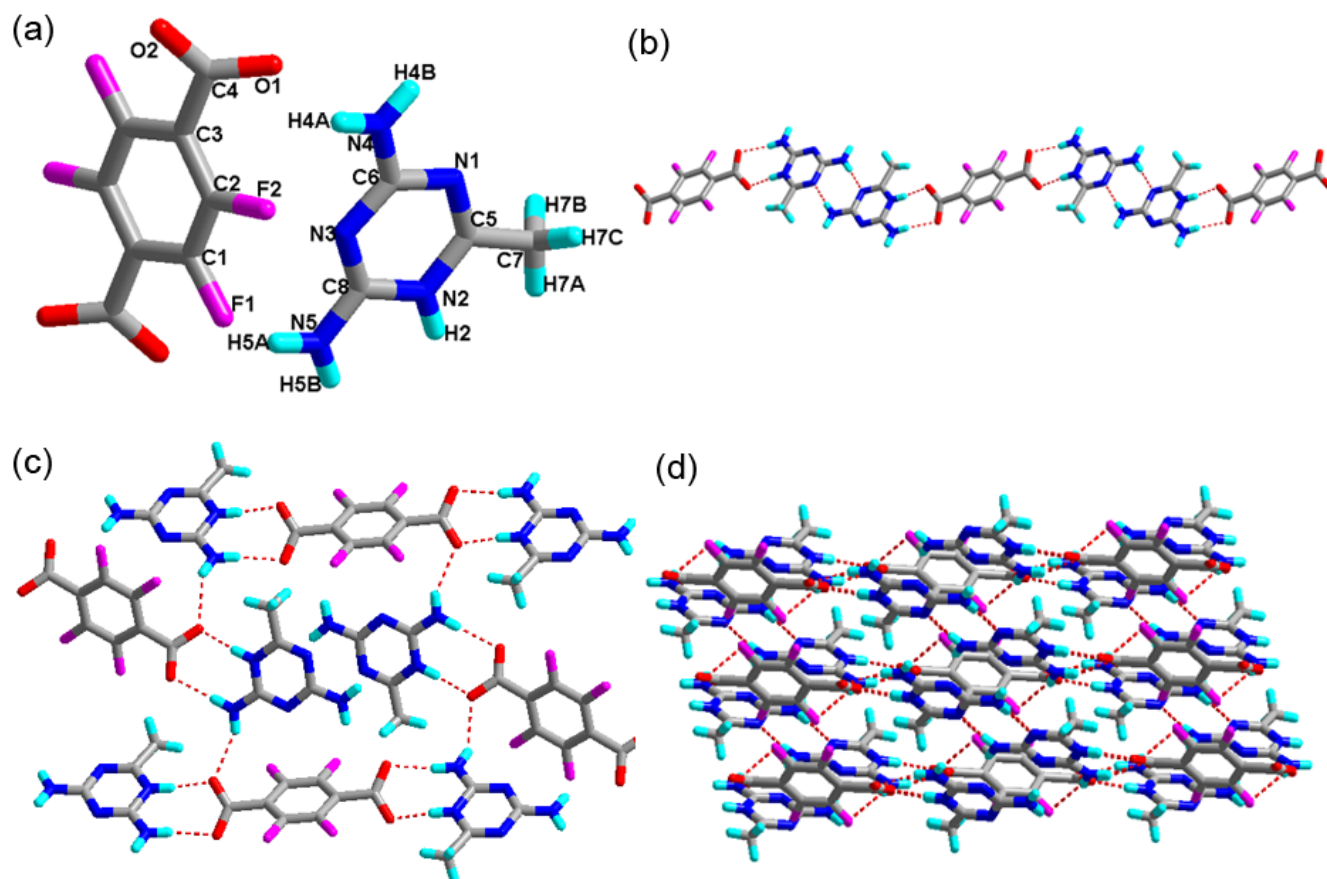


Figure 3. (a) Molecular structure of **3** with atom labeling of the asymmetric unit; (b) 1D supramolecular tape via hydrogen bonds (the hydrogen bonds are indicated as broken lines in this and the subsequent figures); (c) Perspective view of the 2D hydrogen-bonded layer; (d) the resultant 3D network

Tetrafluoroterephthalic acid/2,4-diamino-6-methyl-1,3,5-triazine (1:1), (H_2tfBDC/dmt) Crystal structure of compound **3** crystallizes in the orthorhombic space group $P2(1)/n$ ($Z=2$) with half of the host molecule of H_2tfBDC which is absolutely deprotonated and one molecule of protonated dmt in the asymmetric unit which is displayed in Figure 3a. The H_2tfBDC molecule appears to fully deprotonated phenomenon and the hydroxyl proton transferred to the molecule of 2,4-diamino-6-methyl-1,3,5-triazine, dmt molecules are protonated. The C-O bond lengths should be equal (C4-O2, C4-O1, 1.248Å, 1.234Å, respectively) because of resonance and other electronic perturbations. The exocyclic bond length C3-C4 is elongated to 1.507Å, which is longer than those of cyclic C-C bonds (average 1.375Å) The bond lengths C-F is average 1.335Å. The planes of carboxylic groups (O1/C2/O4) and the benzene ring are 28.776(1)°. While in another H_2tfBDC molecule, the dihedral angles are 12.752(1)° and 22.326(1)°, respectively. The dihedral angles between carboxylic groups of the H_2tfBDC and the benzene ring of the H_2tfBDC are 38.542(1)° and 38.542(9)°, respectively. The two carboxylic groups are almost parallel. The dihedral angle between the benzene ring of H_2tfBDC dianion and the triazine plane of dmt is 69.287(5)°.

Charmingly, neighboring protonated dmt molecules via the N4-H4B...N1 (2.148Å) forms a hydrogen bonded $R^2_2(8)$ dimer (shown in the Scheme 2). The oxygen of the carboxylic group of tetrafluoroterephthalic acid linked the dimers through the N-H...O

hydrogen bonds shape one-dimensional chain (Fig.3b). The distance of the N2-H2...O2 and N5-H5B...O1 hydrogen bonds are determined as 1.783 and 1.995Å, respectively. Furthermore, the hydrogen bonds N5-H5A...O2 connect adjacent chains to form a two-dimensional (2D) layer structure displayed in Figure 3c. The three-dimensional packing architecture is obtained through the N5-H5A...O2 and N5-H5A...F1 hydrogen bonds which are linked the neighboring 2D layers. Synthons $R^2_2(15)$, $R^2_2(8)$, $R^2_2(11)$ and $R^4_8(24)$ are appeared reasonable and shown in Scheme 2.

Tetrafluoroterephthalic acid/Benzoguanamine (1:1), (H_2tfBDC/bga) Crystal structure of compound **4** shows half a molecule of H_2tfBDC , half a dianion of H_2tfBDC and one monocation of benzoguanamine in the asymmetric unit which is depicted in the Figure 4a. The hydroxyl proton transferred to the benzoguanamine molecule thus the bga displays monocation. The state of the carboxylic moiety (neutral or ionic) can be found through the lengths of bond C-O and C=O. The distance of the two C-O bonds for the neutral H_2tfBDC molecule are obviously different, the length of C-OH is 1.291Å, while the length of C=O is 1.211Å. However, the two C-O bonds for the H_2tfBDC dianion are very similar which are 1.253Å and 1.228Å, respectively. The exocyclic bond length C2-C16 and C9-C17 are elongated to 1.522 and 1.505Å, longer than the average distance of the cyclic C-C bonds (average 1.384Å). The bond lengths C-F are average 1.344Å. Within bga monocation subunit, the triazine ring deviate by 2.214(1)° from

coplanarity, with the benzene ring of the bga, which shows that the molecule of bga occurs subtle distortion. The dihedral angle between two benzene ring of the two H₂tfBDC is 49.931(1)°.

In compound **4**, O1-H1...O2 hydrogen bond is generated between the adjacent molecule of H₂tfBDC and the distance of the hydrogen bond is determined as 1.725 Å which is obtained one-dimensional chain of the H₂tfBDC. Noticeably, the molecules of bga as a bridge

hydrogen bonds, and the distance of the hydrogen bonds are identified as 2.103 and 2.104 Å, respectively. In addition, the 2D layers obtain a 3D network architecture through the weak hydrogen bonds N2-H2B...F1, C4-H4...F1 and C6-H6...F4. The distance of the hydrogen bonds are measured as 2.472, 2.527 and 2.678 Å, respectively. Synthons R²₂(8), R²₂(12), R⁴₄(14), R⁴₄(25), R⁴₄(30), and R⁶₆(27) are appeared reasonably and shown in Scheme 2

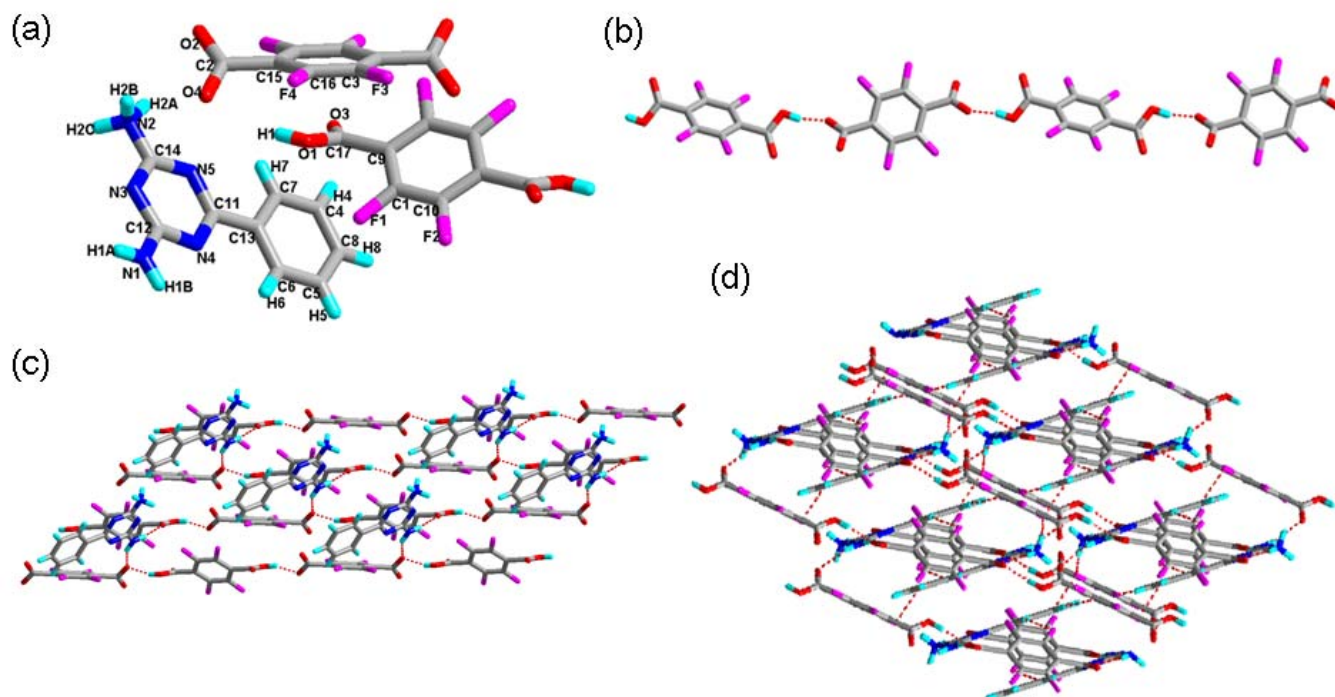


Figure 4. (a) Molecular structure of **4** with atom labeling of the asymmetric unit; (b) 1D supramolecular tape via hydrogen bonds (the hydrogen bonds are indicated as broken lines in this and the subsequent figures); (c) Perspective view of the 2D hydrogen-bonded layer; (d) the resultant 3D network

Tetrafluoroterephthalic acid/2-Methylbenzimidazole (H₂tfBDC/2-MeBzImH) The tetrafluoroterephthalic acid-2-methylbenzimidazole salts crystallizes in the monoclinic space group *C2/c* (*Z*=4) with one and a half molecule of 2-Methylbenzimidazole, half of the dianion of H₂tfBDC, and one molecule of the monoanion of H₂tfBDC in the asymmetric unit. The hydrogen of hydroxy which originally belongs to H₂tfBDC transferred to the 2-MeBzImH. The asymmetric unit is displayed in Figure 5a. The lengths of the two C-O bonds for H₂tfBDC are very different (1.249 Å/1.220 Å/1.283 Å/ for C17-O6/C17-O2/C10-O3 and 1.209 Å for C10=O3) demonstrating that H₂tfBDC is mono-protonated. The distance of the exocyclic bond C1-C10 and C12-C17 are elongated to 1.515 Å and 1.526 Å. In the dianion of H₂tfBDC molecule, the exocyclic bond length C2-C14 is elongated to 1.528 Å, longer than the cyclic those of C-C bonds (average 1.383 Å). The bond lengths C-N and C-F are average 1.354 Å and 1.338 Å, respectively. The dihedral angles between benzene ring is almost co-planar to the benzene ring of the 2-MeBzImH molecule.

The molecules of H₂tfBDC anion through O-H...O hydrogen bonds lead to one-dimensional chains (shown in Fig 5b). Adjacent 1D chains are connected by the molecules of 2-MeBzImH via the N-H...O and C-H...F hydrogen bonds, thus, 2D planar layered structure are formed, meanwhile, synthons R²₂(10), R⁴₃(17), and

R⁴₄(21) result from the hydrogen bonds. Moreover, in this compound, there are another 2D layer structure, unlike the former layer, in this 2D construction, the carboxylic acid are completely protonated, for this reason, the molecules of H₂tfBDC can not form one-dimensional chains, this is the most different from the previous 2D layer, which is displayed in the Figure 5b and 5c. These two kinds of different 2D layers are linked through the hydrogen bonds of C5-H5C...O6, C5-H5C...O3, C5-H5B...O1, and C7-H7C...O2, which distance are determined as 2.645, 2.679, 2.688, 2.697 Å, respectively, to form the three-dimensional network shown in the Figure 5d. Synthons S(6), R⁴₄(15) are emerged reasonably and displayed in the Scheme 2.

Tetrafluoroterephthalic acid/1,4-bis(imidazol) butane (H₂tfBDC/bimb) Crystal structure of compound **6** is refined in the triclinic, *P* $\bar{1}$ space group with one molecule of monoanion of H₂tfBDC and half molecule of dication bimb in the asymmetric unit (*Z*=2) and displayed in the Fig.6a. The lengths of C-O and C=O bonds for H₂tfBDC are obviously different (1.292 Å for C-OH and 1.202 Å for C=O), the lengths of C-O bonds for the other carboxylic group are almost similar (1.253 Å and 1.226 Å). The exocyclic bond lengths C6-C7 and C3-C8 are elongated to 1.526 Å and 1.518 Å, while the cyclic bond lengths C-C are average 1.383 Å, the C-N are average 1.349 Å. The exocyclic bond lengths C-F are average 1.342 Å. The dihedral angle between the two carboxylic groups and the

benzene ring of H₂tfBDC are 38.823(1)° and 45.011(1)°, respectively. In the molecule of bimb, the two imidazole rings are almost parallel, while the dihedral angles between the two imidazole rings and the benzene ring for H₂tfBDC are 34.725(2)° and 34.698(2)°, respectively.

The one-dimensional chains have the same hydrogen bonds with the crystal of **5** except that the connection type, because of the H₂tfBDC molecules present inclined arrangement in the compound **5**, nevertheless, in the structure of form **6**, the molecules of H₂tfBDC demonstrate straight line configuration, thus, the O-H...O hydrogen

bonds in the chains of form **5** are linked staggered while the same hydrogen bonds in form **6** are connected parallel (shown in Fig.6b). Synthons R²₂(11) and R⁴₆(25) participate in forming the two-dimensional layers which is shown in the Fig.6c, furthermore, the stronger hydrogen bonds N-H...O with the weaker hydrogen bonds C-H...F link the adjacent 2D layers to a three-dimensional packing network (shown in Fig.6d), in this structure contains the synthons R⁴₄(24). In addition, synthons S(4), R³₃(18), R²₄(8), R²₄(12) are emerged reasonably and displayed in the Scheme 2

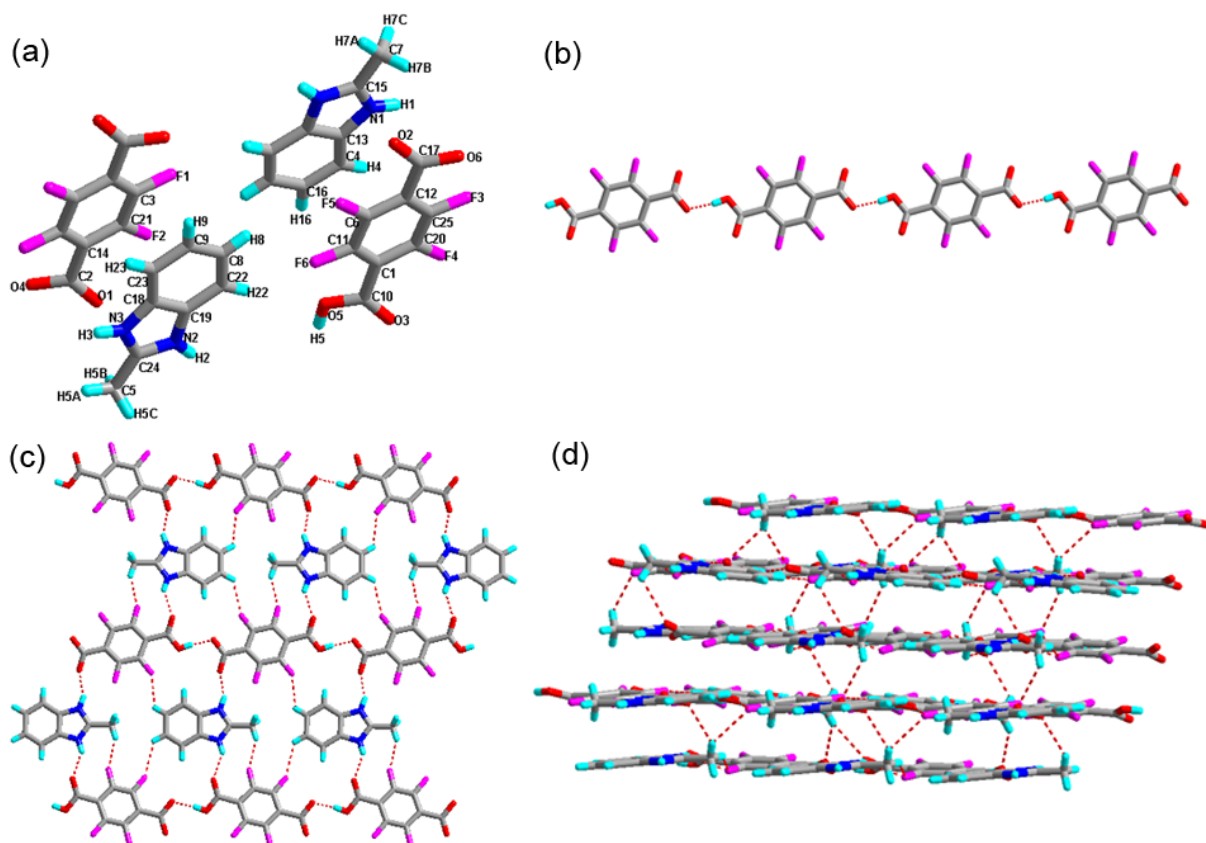


Figure 5 (a) Molecular structure of **5** with atom labeling of the asymmetric unit; (b) 1D supramolecular tape via hydrogen bonds (the hydrogen bonds are indicated as broken lines in this and the subsequent figures); (c) Perspective view of the 2D hydrogen-bonded layer; (d) the resultant 3D network

Tetrafluoroterephthalic acid/2-amino-4-hydroxy-6-methyl pyrimidine (H₂tfBDC/ahmp) Crystallographic analysis of the crystal of **7** is monohydrate and shows it to contain half crystallographically independent molecule of H₂tfBDC, half molecule of dianion H₂tfBDC, one molecule of H₂O, and one molecule of monocation 2-amino-4-hydroxy-6-methyl pyrimidine in the monoclinic, *P*2(1)/*n* space group (*Z*=4). Figure 7a shows asymmetric unit. The exocyclic bond lengths C12-C18, C24-C25 and C15-C16 are elongated to 1.518Å, 1.503Å and 1.495Å. The cyclic bond lengths C-C and C-N are average 1.385Å and 1.362Å, respectively. The distance of the bonds C-F is average 1.343Å. The distance of two C-O bonds for H₂tfBDC are significantly different (1.299Å for C-OH and 1.198Å for C=O), however, the two C-O bonds for H₂tfBDC dianion are almost similar (1.250Å and 1.245Å)

showing that one of H₂tfBDC is neutral and the other one is fully deprotonated. Within the two H₂tfBDC molecules, the dihedral angles between carboxylic groups and the benzene ring of H₂tfBDC are 41.264(3)° and 40.115(1)°, respectively. The dihedral angle between the two H₂tfBDC molecules is 56.205(3)°.

In the crystal of **7**, water molecules play an important role in forming the structure and interact with H₂tfBDC via O4-H4...O6 and O6-H6A...O2 hydrogen bonds to form a wavelike chain which is shown in Fig.7b. In which the distance of the hydrogen bonds is 1.721 and 1.886Å, respectively. The molecules of 2-amino-4-hydroxy-6-methyl pyrimidine intersperse in the adjacent one-dimensional chains. Layers are formed by the chains and displayed in the Figure 7c in which the chains are connected by the 2-amino-4-hydroxy-6-methyl pyrimidine molecules through the N3-

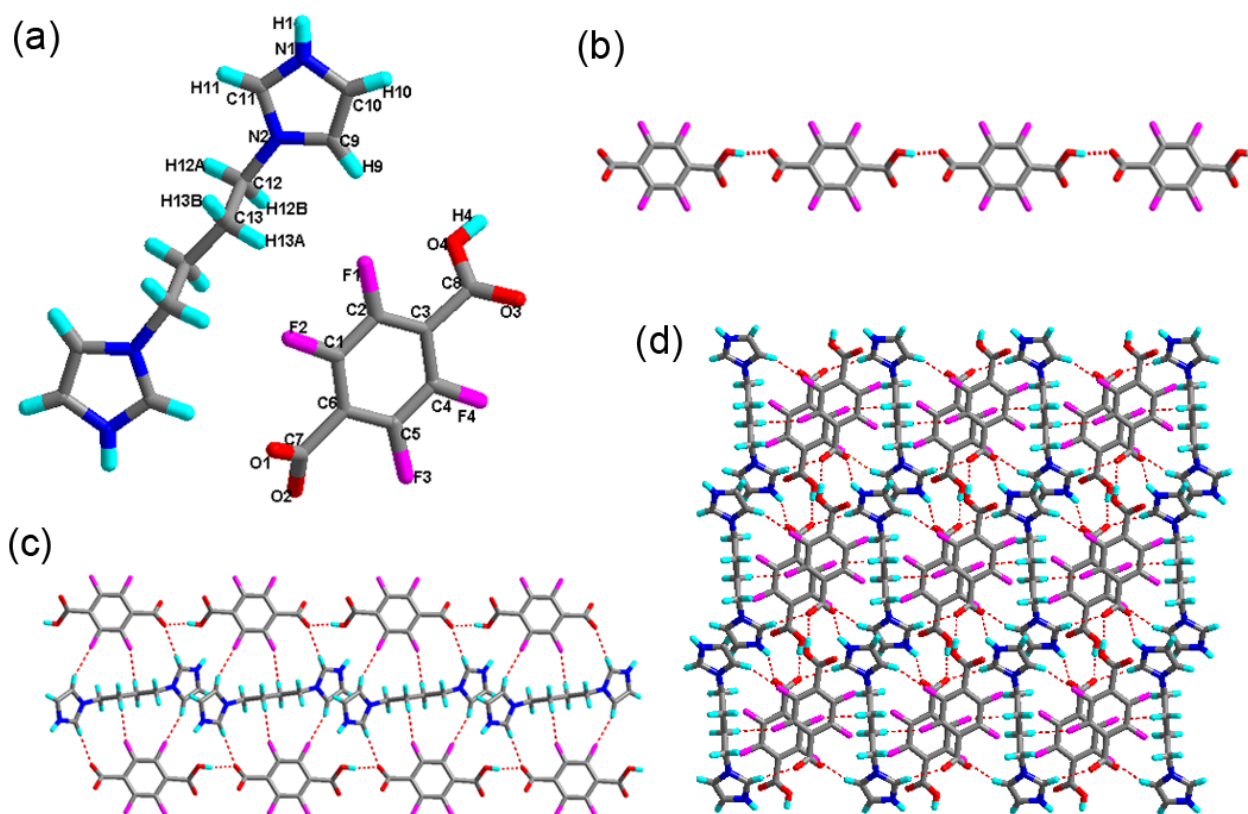


Figure 6 (a) Molecular structure of **6** with atom labeling of the asymmetric unit; (b) 1D supramolecular tape via hydrogen bonds (the hydrogen bonds are indicated as broken lines in this and the subsequent figures); (c) Perspective view of the 2D hydrogen-bonded layer; (d) the resultant 3D network

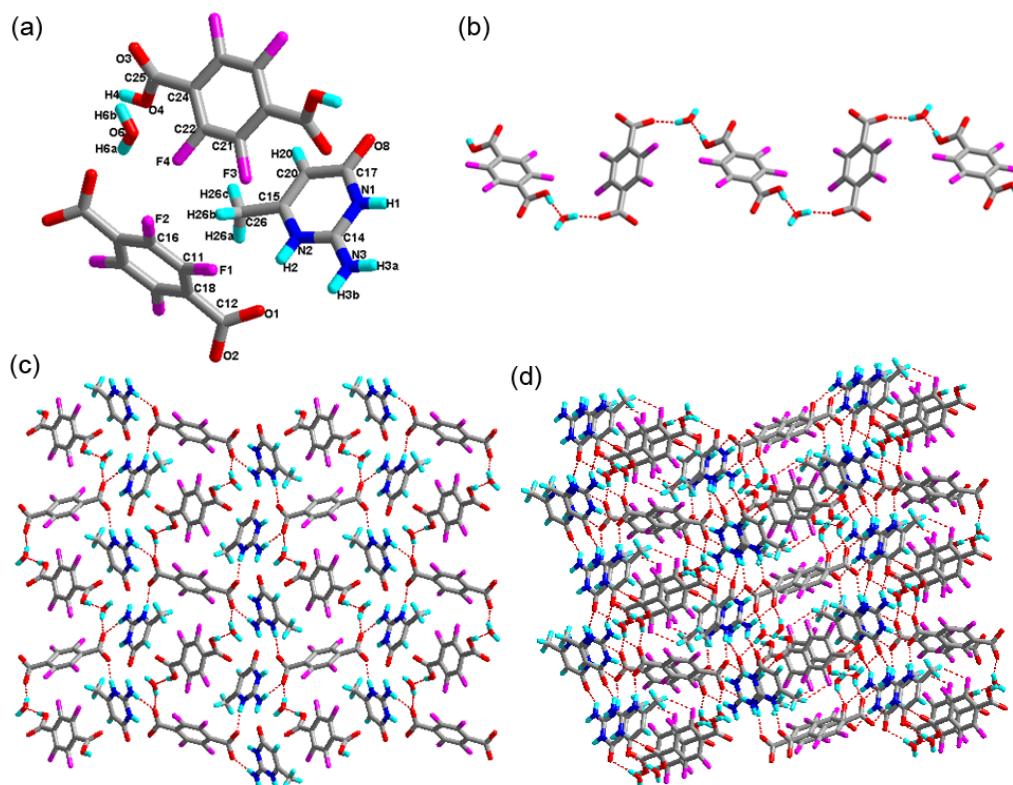


Figure 7 (a) Molecular structure of **7** with atom labeling of the asymmetric unit; (b) 1D supramolecular tape via hydrogen bonds (the hydrogen bonds are indicated as broken lines in this and the subsequent figures); (c) Perspective view of the 2D hydrogen-bonded layer; (d) the resultant 3D network

H3B \cdots O2(1.905Å) and N2-H2 \cdots O1(1.934Å) hydrogen bonds. As a consequence, these 2D sheets are extended to a three-dimensional network (shown in the Figure 7d) through the hydrogen bonds C20-H20 \cdots O3 and weak hydrogen bonds C26-H26B \cdots F4 which the distance is 2.419 and 2.577Å, respectively. New hydrogen-bonded patterns labeled as S(6), R²₂(8), R²₄(8) and R²₃(10) come into being and display in Scheme 2

Tetrafluoroterephthalic acid/1,2-bis[(2-methylimidazol-1-yl)methyl] benzene (H₂tfBDC/L7) In regard to compound **8**, it is monohydrate as the same with crystal of **7**. In the structure of **8**, crystallizing in the monoclinic space group *P*2(1)/*c*, the asymmetric unit is consisted of two tetrafluoroterephthalic acid monoanion, one L7 dication, and one water molecule. The exocyclic bond lengths C27-C28, C26-C29, C8-C12, C2-C7, C4-C13 and C3-C15 are elongated to 1.532Å, 1.514Å, 1.512Å, 1.524Å, 1.521Å and 1.507Å, longer than the cyclic those of C-C bonds which distance is average 1.377Å. The bond length C-F is average 1.343Å, and the distance of the C-N is average 1.353Å. Within L7 subunit, the dihedral angles between two imidazole rings and the benzene ring are 76.079(2)° and 88.438(2)°, respectively. Moreover, the two imidazole groups

are located in the same side of the plane of benzene ring. The dihedral angle between the two H₂tfBDC molecules is 66.311(1)°.

Compared with the one-dimensional chains of the compound **7**, in crystal of **8**, the H₂tfBDC monoanions are self-assembled into a supramolecular chain (shown in Fig.8a) via O4-H4 \cdots O1 hydrogen bonds, and the distance of hydrogen bonds is 1.692Å without water molecules. These 1D supramolecular chains are further connected through the N1-H1 \cdots O1, N4-H4 \cdots O1W hydrogen bonds, and the weak hydrogen bonds C21-H21 \cdots F8 to produce a two-dimensional sheets structure (shown in Fig. 8b). furthermore, in this 2D supramolecule structure, water molecules disperse into two hydrogen bonds embedded in two-dimensional structure. Not only that, the L7 molecules as a polydentate ligand also play a meaningful role in bridging, they connect the 1D chains and the water molecules to form a stable 2D layer (Fig.8c). Each such 2D layer running along *c* axis via C-H \cdots O hydrogen bonds (C19-H19 \cdots O3, C4-H4B \cdots O7, C15-H15B \cdots O3, and C4-H4A \cdots O2), thereby generating a 3D network which is displayed in the Figure 8d. Seven types of hydrogen-bonded patterns, indicated as S(6), R²₂(11), R³₃(11), R²₄(16), R⁵₅(18), and R⁶₈(29) synthons, are emerged reasonable and displayed in the Scheme 2

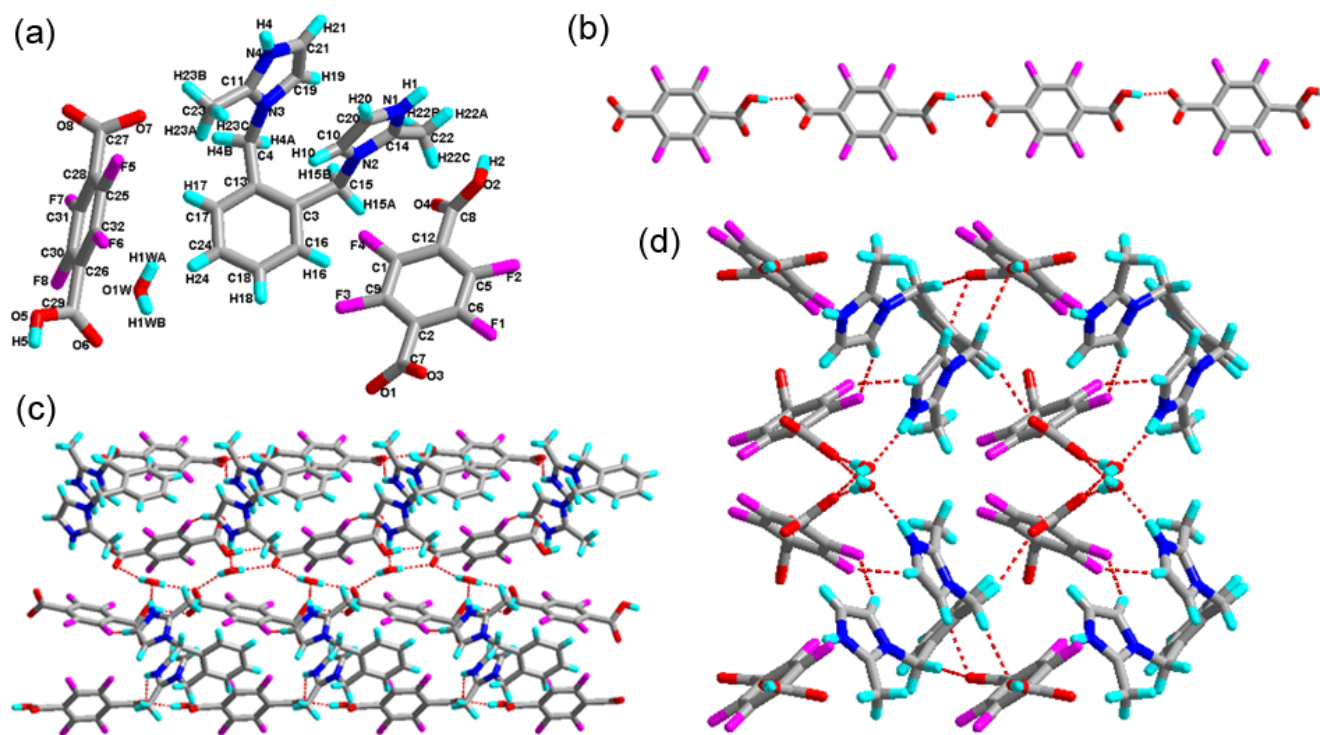


Figure 8 (a) Molecular structure of **8** with atom labeling of the asymmetric unit; (b) 1D supramolecular tape via hydrogen bonds (the hydrogen bonds are indicated as broken lines in this and the subsequent figures); (c) Perspective view of the 2D hydrogen-bonded layer; (d) the resultant 3D network

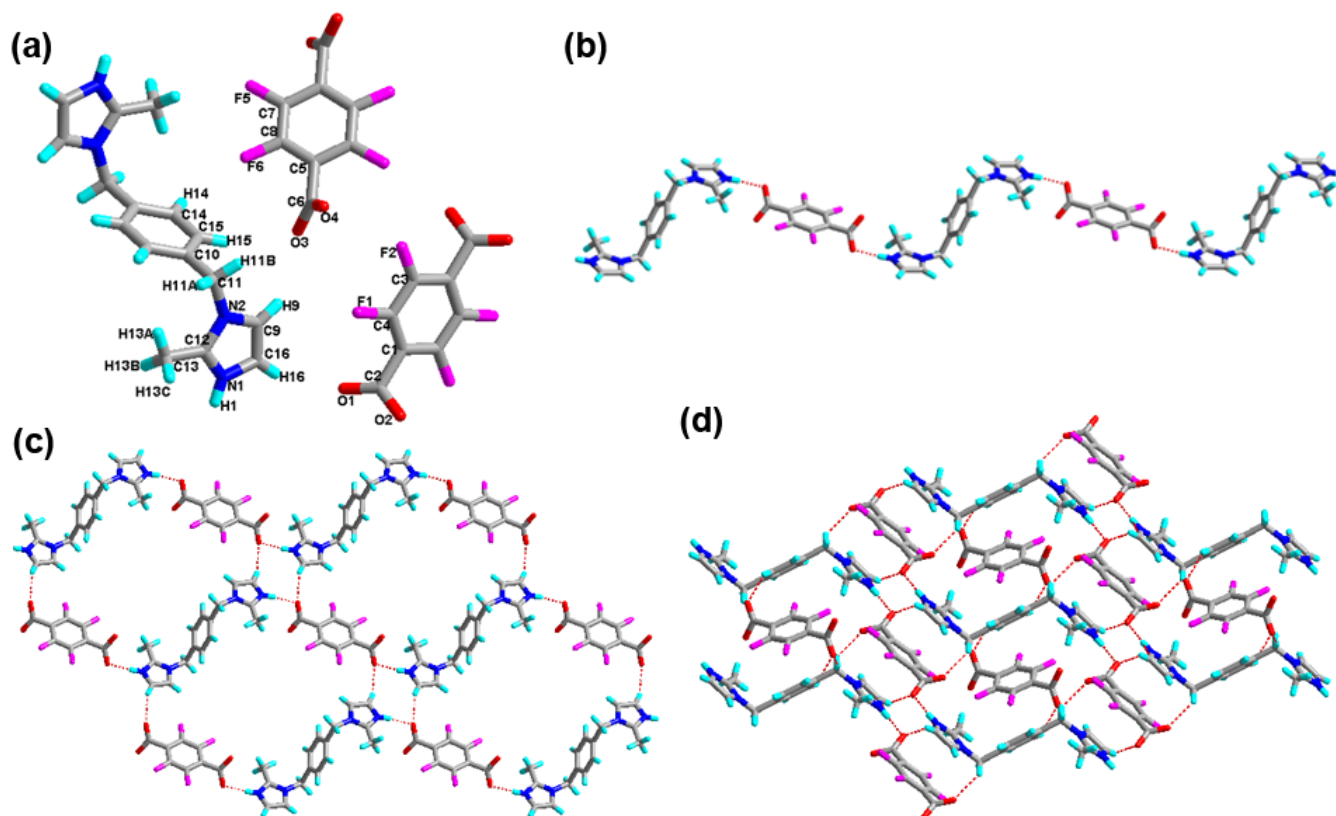


Figure 9 (a) Molecular structure of **9** with atom labeling of the asymmetric unit; (b) 1D supramolecular tape via hydrogen bonds (the hydrogen bonds are indicated as broken lines in this and the subsequent figures); (c) Perspective view of the 2D hydrogen-bonded layer; (d) the resultant 3D network

Tetrafluoroterephthalic acid/1,4-bis[(2-methylimidazol-1-yl)methyl] benzene (H_2 tfBDC/L5) Complex **9** crystallizes in the triclinic crystal system in the space group $P\bar{1}$. Figure 9a shows the asymmetric unit consists of half a L5 dication and halves of two H_2 tfBDC monoanion, out of which H_2 tfBDC molecules transfer their protons to the imidazole ring of L5, resulting in a H_2 tfBDC-L5 salt. The exocyclic bond lengths C5-C6, C1-C2 and C10-C11 are elongated to 1.519Å, 1.524Å and 1.509Å, longer than the cyclic those of C-C bonds (average 1.380Å). Similarly, the exocyclic bond length C11-N2 is elongated to 1.470Å longer than the cyclic bond length C-N bonds (average 1.356Å). The distance of the C-F is average 1.340Å. The dihedral angle between the two H_2 tfBDC molecules is 53.596(1)°, meanwhile, within the L5 subunit, the two imidazole rings almost parallel, and they make dihedral angles of 71.105(2)° and 71.284(2)°, respectively, with the central benzene ring.

In the crystal lattice of compound **9**, one-dimensional chain formed by N1-H1...O1 interactions are present in the Figure 9b. In this 1D structure, due to two imidazole rings in the L5 toward two different sides respectively, the chain demonstrates like a wave. Synthons $R_2^4(10)$ and $R_4^4(28)$ interact to form a two-dimensional layer, which is displayed in Figure 9c, in this architecture, the synthons $R_2^4(10)$ and $R_4^4(28)$ are formed by the hydrogen bonds: N1-H1...O1 and C16-H16...O1, and the distance of the hydrogen bonds is 1.818 and 2.460Å, respectively. Adjacent 2D sheets through the C11-H11A...O3 hydrogen bonds to form a three-dimensional network which is displayed in the Figure 9d. In addition, synthons

$S(8)$ and $R_4^4(18)$ are emerged legitimately and shown in the Scheme 2.

Thermal stability analysis

All compounds **1-9** are stable in air and can maintain their structural integrity at ambient conditions for a long time. In order to examine the thermal stability of all compounds, the TGA and DSC were carried out between 0 and 900°C in nitrogen atmosphere. The DSC traces and TGA data for the crystals are presented in Supporting Information.

TGA experiments were implemented to investigate their thermal stability. The behaviors of the nine compounds are depicted in Figure 10. As for **7**, the TGA results indicate that they remain intact until 245°C, and then there are a sharp weight loss ending at 297°C. (peaks: 251°C for crystal **7**), corresponding to the explosion of all base and acid components and which is showed in Fig 10. The weight loss of compound **7** up to 99.13% to 298°C. The TGA curves of **1** and **2** indicate that there are two consecutive weight losses of the two samples. Compound **1** decomposes from 120°C to 257°C (peaking at 171°C and 219°C, respectively), while **2** is less stable than the compound **1** and when it comes to 110°C the decomposition of the framework begins. (peaking at 154°C and 248°C, respectively). As for **1**, the first weight loss of 31.40% from 120 to 185°C (calculated: 35.29%) corresponds to the loss of one 2,3-dimethyl pyrazine molecule per formula. The second weight loss of 66.68% (calculated: 64.71%) can be detected from 186 to 257°C, which is owed to decomposition of

tetrafluoroterephthalic acid molecule. Compared with compound 1, the TGA measurement of 2 shows a weight loss of 30.51% in the temperature range 110°C to 155°C, which corresponds to the loss of 2,6-dimethyl pyrazine molecule, and the second weight loss represented the loss of acid components (calculated: 64.71%, found: 69.32%). The TGA measurement of 3 indicates that the compound does not melt and is stable up to 186°C, at which temperature the crystal begins to decompose. The ligand 2,4-diamino-6-methyl-1,3,5-triazine and tetrafluoroterephthalic acid molecule decompose at 186-282°C with two peaks at 231°C and 255°C. As for 3, the first weight loss of 15.50% from 186 to 241°C, and the second weight loss of 83.99% from 187 to 255°C. For compound 4 and 5, two consecutive weight losses of all substance in the 150°C-270°C (peaking at 172°C, 247°C, and 153°C, 205°C, respectively). The first two mass losses stand for the loss of base component of 4 and a small part of base component of 5 (calculated: 48.83%, found: 41.87% for 4; calculated: 47.42%, found: 4.58% for 5), and the second two mass losses represented the remaining ingredients. The TGA curve of compounds 6, 8 and 9 indicate that they have the similar trend of decomposition. They are stable up to 170°C at which temperature they start to melt and decompose. The curves show two consecutive weight losses of the three crystalline samples from 170 to 300 °C (peaking at 165°C and 259°C for 6, 167 and 280°C for 8, and 174°C and 287°C for 9, respectively.). In 6, 8 and 9, the first mass losses illustrated the loss of base components which is same with the compounds 4 and 5, and the second mass losses represented the acid molecules. Moreover, the theoretical value and practical value differ within a reasonable range. Broadly speaking, the nine frameworks have a remarkably thermal stability.

Conclusions

A series of new organic multi-component molecular solids based on H₂tfBDC and N-containing heterocycles have been synthesized by varying molar ratio under different solvent conditions and determined thoroughly by single crystal X-ray diffraction, IR, and TGA. It has been proven that H₂tfBDC is a good candidate for constructing supramolecular structures with N-containing heterocycles. Through analyzing the 3D supramolecular architectures show that the formation of the organic solids is mainly influenced by the strong hydrogen bonds N-H...O, O-H...O, and N-H...N. Meanwhile, the weak intermolecular interaction C-H...F and C-H...O are critical important in directing the molecular assembly especially used for constructing 3D network when it lacks of strong H-bonds. The hydrogen bonding C-H...F exists in all nine compounds, several novel synthons based on C-H...F have been observed in this structures.

Our intention is to find out the capability of “organic fluorine” in constructing the crystal structures, and the role of C-H...F has been well presented. But, we are disappointed that we can't discover the F...F interaction. We will introduce other halogens and some related functional groups to understand the

halogen...halogen interactions in the organic solids, and this direction will be in progress in our laboratory.

Acknowledgements

This work was supported by the National Natural Science Foundation of China (No. 51372125 and 21203106), and the Natural Science Foundation of Shandong Province, China (No. ZR2011BL015).

Notes and references

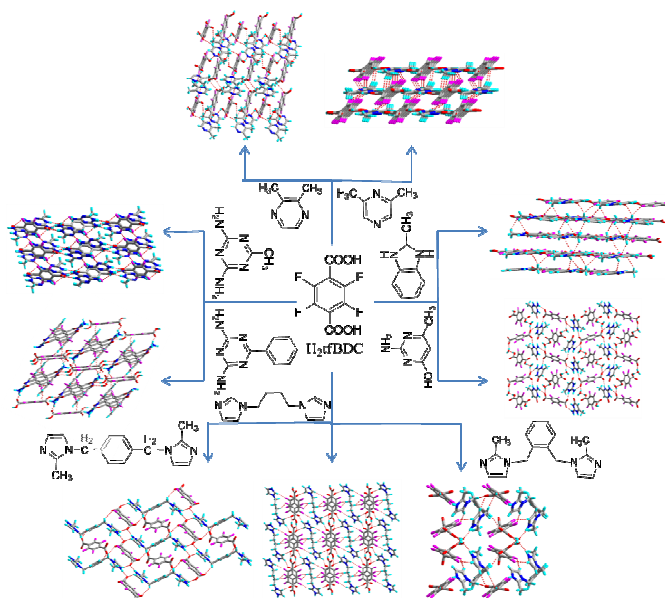
- (a) S. H. Long, P. P. Zhou, S. Parkin, and T. L. Li, *Cryst. Growth Des.*, 2013, dx.doi.org/10.1021; (b) A. Putta, J. D. Mottishaw, Z. H. Wang, and H. Sun, *Cryst. Growth Des.*, 2013, dx.doi.org/10.1021; (c) A. R. Choudhury and T. N. Guru Row, *CrystEngComm*, 2006, **8**, 265-274; (d) A. Jacobs, L. R. Nassimbeni, G. Ramon, and B. K. Sebogisi, *CrystEngComm*, 2010, **12**, 3065-3070; (e) A. R. Choudhury and T. N. Guru Row, *Cryst. Growth Des.*, 2004, **4**, 47-52; (f) H. B. Zhang, C. Y. Guo, X. C. Wang, J. J. Xu, X. He, Y. Liu, X. F. Liu, H. Huang, and J. Sun, *Cryst. Growth Des.*, 2013, **13**, 679-687; (g) M.A.Elbageema, H. G. M. Edwards, T. Munshi, M. D. Hargreaves, P. Matousek, and I. J. Scowen, *Cryst. Growth Des.*, 2010, **10**, 2360-2371; (h) D. Wang, R. Yu, N. Kumada, and N. Kinomura, *Chem. Mater.*, 2000, **12**, 956-960.
- (a) G. R. Desiraju, *J. Am. Chem. Soc.*, 2013, **135**, 9952-9967; (b) S. Tothadi, S. Joseph, and G. R. Desiraju, *Cryst. Growth Des.*, 2013, **13**, 3242-3254; (c) L. Rajput, P. Sanphui, and G. R. Desiraju, *Growth Des.*, 2013, **13**, 3681-3690; (d) V. R. Hathwar, T. S. Thakur, T. N. Guru Row, and G. R. Desiraju, *Cryst. Growth Des.*, 2011, **11**, 616-623; (e) G. R. Desiraju, *Growth Des.*, 2011, **11**, 896-898.
- (a) D. Uraguchi, Y. Ueki, and T. Ooi, *Science*, 2009, **326**, 120; (b) A. Mukherjee, and G. R. Desiraju, *Cryst. Growth Des.*, 2011, **11**, 3735-3739; (c) A. G. Dikundwar, R. Sathiskumar, T. N. Guru Row, and G. R. Desiraju, *Cryst. Growth Des.*, 2011, **11**, 3954-3963;
- (a) I. D. Madura, K. Czerwińska, M. Jakubczyk, A. Pawelko, A. A. Woźniak, and A. Spożyński, *Cryst. Growth Des.*, 2013, dx.doi.org/10.1021; (b) C. B. Aakeröy, P. D. Chopade, C. Ganser, and J. Desper, *Chem. Commun.*, 2011, **47**, 4688-4690.
- (a) L. Rajput, N. Jana, and K. Biradha, *Cryst. Growth Des.*, 2010, **10**, 4565-4570; (b) M. D. Prasanna and T. N. Guru Row, *J. Mol. Struct.*, 2001, **562**, 55-61; (c) S. S. Kuduva, D. C. Craig, A. Nangia, and G. R. Deairaju, *J. Am. Chem. Soc.*, 1999, **121**, 1936-1944; (d) D. Wang, R. Yu, T. Takei, N. Kumada, N. Kinomura, A. Onda, K. Kajiyoshi, and K. Yanagisawa, *Chem. Lett.*, 2002, 398-399; (e) D. Wang, R. Yu, N. Kumada, N. Kinomura, K. Yanagisawa, Y. Matsumura, and T. Yashima *Chem. Lett.*, 2002, 804-805.
- (a) K. M. Dethlefs and P. Hobza, *Chem. Rev.*, 2000, **100**, 143-167; (b) W. L. Delano, *J. Mol. Struct.*, 2002, **12**, 14-20; (c) G. Cuniberti, G. Fagas, and K. Richter, *Springer*, 2005, **680**, 1-10; (d) A. Lmberty and S. Pérez, *Chem. Rev.*, 2000, **100**, 4567-4588.
- (a) S. Kitagawa, R. Kitaura, and S. Noro, *Angew. Chem. Int. Ed.*, 2004, **43**, 2334 -2375; (b) C. B. Aakeröy, N. C. Schultheiss, A. Rajbanshi, J. Desper, and C. Moore, *Cryst. Growth Des.*, 2009, **9**, 432-441; (c) D. A. McMorran, *Inorg. Chem.*, 2008, **47**, 592-601; (d) Y. X. Lu, Y. T. Liu, H. Y. Li, X. Zhu, H. L. Liu, and W. L. Zhu, *J.*

- Phys. Chem. A*, 2012, **116**, 2591-2597; (e) P. Zhou, J. W. Zou, F. F. Tian and Z. C. Shang, *J. Chem. Inf. Model.*, 2009, **49**, 2344-2355.
- 8 (a) N. Borho and Y. J. Xu, *J. Am. Chem. Soc.*, 2008, **130**, 5916-5921; (b) H. Y. Gao, X. R. Zhao, H. Wang, X. Pang, and W. J. Jin, *Cryst. Growth Des.*, 2012, **12**, 4377-4387; (c) Z. H. Zhang, S. C. Chen, M. Y. He, C. Li, Q. Chen, and M. Du, *Cryst. Growth Des.*, 2011, **11**, 5171-5175; (d) R. Yu, D. Wang, T. Takei, H. Koizumi, N. Kumada, and N. Kinomura, *J. Solid State Chem.*, 2001, **157**, 180-185; (e) R. Yu, D. Wang, N. Kumada, and N. Kinomura, *Chem. Mater.*, 2000, **12**, 3527-3529.
- 9 (a) K. Reichenbacher, H. I. Süss, and J. Hulliger, *Chem. Soc. Rev.*, 2005, **34**, 22-30; (b) S. K. Nayak, M. K. Reddy, T. N. Guru Row, and D. Chopra, *Cryst. Growth Des.*, 2011, **11**, 1578-1596.
- 10 S. Purser, T. D. W. Claridge, B. Odell, P. R. Moore, and V. Gouverneur, *Org. Lett.*, 2008, **10**, 4263-4266.
- 11 (a) R. E. Cobblestick and R. W. H. Small, *Acta Cryst.*, 1972, **B28**, 2924-2928; (b) S. L. Staun and A. G. Oliver, *Acta Cryst.*, 2012, **C68**, o84-o87.
- 12 Z. Hulvey, J. D. Furman, S. A. Turner, M. Tang, and A. K. Cheetham, *Cryst. Growth Des.*, 2010, **10**, 2041-2043
- 13 (a) A. Abad, C. Agulló, A. C. Cuñat, C. Vilanova, and M. Carmen Ramírez de Arellano, *Cryst. Growth Des.*, 2006, **6**, 45-57; (b) D. Chopra and T. N. Guru Row, *Cryst. Growth Des.*, 2006, **6**, 1267-1270; (c) J. Ridout and M. R. Probert, *Cryst. Growth Des.*, 2013, dx.doi.org/10.1021; (d) V. R. Hathwar, T. S. Thakur, R. Dubey, M. S. Pavan, T. N. Guru Row, *J. Phys. Chem. A*, 2011, **115**, 12852-12863.
- 14 (a) G. Asensio, M. Medio-Simon, P. Alemán, and C. Ramírez de Arellano, *Cryst. Growth Des.*, 2006, **6**, 2769-2778; (b) V. Vasylieva and K. Merz, *Cryst. Growth Des.*, 2010, **10**, 4250-4255.
- 15 (a) S. K. Nayak, M. K. Reddy, T. N. Guru Row, and D. Chopra, *Cryst. Growth Des.*, 2011, **11**, 1578-1596; (b) S. Ghosh, A. R. Choudhury, T. N. Guru Row, and U. Maitra, *Organic Letters*, 2005, **7**, 1441-1444; (c) V. R. Hathwar, T. S. Thakur, R. Dubey, M. S. Pavan, T. N. Guru Row, and G. R. Desiraju, *J. Phys. Chem. A*, 2011, **115**, 12852-12863; (d) N. Lu, R. M. Ley, C. E. Cotton, W. C. Chung, J. S. Francisco, and E. Negishi, *J. Phys. Chem. A*, 2013, **117**, 8256-8262; (e) G. Kaur, P. Panini, D. Chopra, and A. R. Choudhury, *Cryst. Growth Des.*, 2012, **12**, 5096-5110; (f) G. Asensio, M. M. Simon, P. Alemán, and C. R. Arellano, *Cryst. Growth Des.*, 2006, **6**, 2769-2778.
- 16 S. Tothadi, S. Joseph, and G. R. Desiraju, *Cryst. Growth Des.*, 2013, **13**, 3242-3254.
- 17 L. Wang, L. Zhao, Y. J. Hu, W. Q. Wang, R. X. Chen, and Y. Yang, *CrystEngComm*, 2013, **15**, 2835-2852.
- 18 J. F. Ma; J. Yang, G. L. Zheng, L. Li, Y. M. Zhang; F. F. Li, Liu and J. F. Liu, *Polyhedron*, 2004, **23**, 553-559.
- 19 B. F. Hoskins, R. Robson, and D. A. Slizys, *J. Am. Chem. Soc.*, 1997, **119**, 2952-2953.
- 20 (a) G. M. Sheldrick, *SHELXS-97, Program for the Solution of Crystal Structures*, University of Göttingen, Göttingen, Germany, 1997. (b) G. M. Sheldrick, *SHELXL-97, Programs for X-ray Crystal Structure Refinement*, University of Göttingen, Göttingen, Germany, 1997.

Table of contents

Energetic Multi-component Molecular Solids of
Tetrafluoroterephthalic Acid with Some Aza Compounds by
Strong Hydrogen Bonds and Weak Intermolecular Interactions
of C-H \cdots F and C-H \cdots O

Lei Wang^{a*}, Yanjing Hu^a, Wenqiang Wang^a, Faqian Liu^a, and Keke Huang^{b*}



Tetrafluoroterephthalic acid forms nine new crystals with a series of N-containing heterocycles including salts/co-crystals/hydrates were discussed in the context.